AD_____
(Leave blank)

Award Number:

W81XWH-08-1-0431

TITLE:

Biomarker Discovery and Mechanistic Studies of Prostate Cancer Using Targeted Proteomic Approaches

PRINCIPAL INVESTIGATOR:

Natasha Kyprianou, Ph.D.

CONTRACTING ORGANIZATION:

University of Kentucky
Lexington, KY 40536

REPORT DATE:

July 2012

TYPE OF REPORT:

Final

PREPARED FOR: U.S. Army Medical Research and Materiel Command
Fort Detrick, Maryland 21702-5012

DISTRIBUTION STATEMENT: (Check one)

■ Approved for public release; distribution unlimited

□ Distribution limited to U.S. Government agencies only; report contains proprietary information

REPORT DOCUMENTATION PAGE

Form Approved
OMB No. 0704-0188

1. REPORT DATE *(DD-MM-YYYY)*	**2. REPORT TYPE**	**3. DATES COVERED** *(From - To)*
July 2012	Final	1 July 2008 – 30 June 2012

4. TITLE AND SUBTITLE
Biomarker Discovery and Mechanistic Studies of Prostate Cancer Using Targeted Proteomic Approaches

5a. CONTRACT NUMBER

5b. GRANT NUMBER
W81XWH-08-1-0431

5c. PROGRAM ELEMENT NUMBER

6. AUTHOR(S)
Natasha Kyprianou

5d. PROJECT NUMBER

5e. TASK NUMBER

5f. WORK UNIT NUMBER

7. PERFORMING ORGANIZATION NAME(S) AND ADDRESS(ES)

University of Kentucky
Lexington, KY 40536

8. PERFORMING ORGANIZATION REPORT NUMBER

9. SPONSORING / MONITORING AGENCY NAME(S) AND ADDRESS(ES)
U.S. Army Medical Research
And Material Command
Fort Detrick, MD 21702-5012

10. SPONSOR/MONITOR'S ACRONYM(S)

11. SPONSOR/MONITOR'S REPORT NUMBER(S)

12. DISTRIBUTION / AVAILABILITY STATEMENT
Approved for public release

13. SUPPLEMENTARY NOTES

14. ABSTRACT
Our findings reveal that EMMPRIN immunoreactivity was primarily detected among the glandular epithelial cells; EMMPRIN levels progressively increased with increasing age of TRAMP mice (6-27wks); with the highest detected in liver metastases. Quantitative analysis revealed that by 27-wks (an age exhibiting highly aggressive prostate tumor phenotype), EMMPRIN expression increased significantly (P=0.001). These results suggest that EMMPRIN may have diagnostic value in prostate cancer detection in advanced disease.

15. SUBJECT TERMS
EMMPRIN, prostate cancer, metastasis

16. SECURITY CLASSIFICATION OF:			**17. LIMITATION OF ABSTRACT**	**18. NUMBER OF PAGES**	**19a. NAME OF RESPONSIBLE PERSON**
					USAMRMC
a. REPORT	**b. ABSTRACT**	**c. THIS PAGE**	UU	5	**19b. TELEPHONE NUMBER** *(include area code)*
U	U	U			

Standard Form 298 (Rev. 8-98)
Prescribed by ANSI Std. Z39.18

TABLE OF CONTENTS:

DOD Synergistic Grant Annual Report: W81XWH-08-1-0431 (2012)

(Initiating PI: Haining Zhu)

Partnering-PI: Natasha Kyprianou

Introduction: The focus of this collaborative work has been the identification of EMMPRIN, a membrane protein found to be overexpressed in prostate cancer epithelial cells that exhibit a highly metastatic potential. Previous evidence identified the involvement of EMMPRIN in cancer development and progression via controlling extracellular matrix remodeling and anchor independent growth by stimulating MMP production, angiogenesis via VEGF by activation of AKT-PIK3 pathway, and cell invasion by up-regulation of urokinase-type palsminogen activator. The emerging rationale on pursuing the role of EMMPRIN as a functional biomarker in prostate cancer metastasis led us to determine the status of additional proteins that control the actin-cytoskeleton organization, such as cofilin.

Body: Targeting of tumor cell metastasis is of major therapeutic significance and its exploitation may lead to the identification of effective new modulations such as : (**1**) reversing the ability of tumor cells of becoming resistant to anoikis, therefore making them more susceptible to anoikis-inducing agents; (**2**) interfering with the seeding process of tumor cells into secondary places by making tumor cells non-sensitive to the chemotatic and environmental cues of the new target organ; and (**3**) making these secondary targets less “appealing” to the cancer cells by blocking key molecules promoting cancer cell seeding and survival. Membrane proteins play a critical role during the metastasis process since they regulate cell-cell interactions and coordinate cell-tumorenvironment communication. The initiating PI supported by this PCRP Synergistic Grant (USAMRMC PC074317), Dr. Zhu by utilizing proteomic approaches, identified EMMPRIN as one of differentially expressed membrane proteins in prostate cells, revealing considerably higher levels of EMMPRIN protein in highly metastatic human prostate cancer cells. Subsequent validation studies in Dr. Kyprianou’s lab led to the identification of

additional proteins that regulate the cytoskeleton organization as potential regulators of prostate cell migration, cell-cell interactions and ultimately invasion and metastasis.

(1) Ongoing Work: The current focus is on a) the mechanistic dissection of EMMPRIN's contribution to metastasis and b) the significance of EMMPRIN in human prostate cancer progression to metastastic disease and clinical outcomes to define the potential value of this player as a marker of metastasis, studies will pursue expression profiling of EMMPRIN proteein levels in a series of human prostate cancer specimens of increasing Gleason grade and metastastic lesions. Human prostate tissue specimens from patients with primary and metastatic prostate tumors (Department of Pathology, University of Pittsburgh), were subjected to immuno-profiling for EMMPRIN expression and quantitative analysis will be achieved using computer-image analysis in normal prostate; benign prostate hyperplasia, BPH; prostate primary tumors (Gleason Score range 6-9); and metastatic lesions (n=45). Ongoing translational studies focus on establishing a correlation between EMMPRIN expression with serum PSA levels, Gleason grade and patient (disease-free) survival in a large cohort of prostate cancer patients, which may define the value of EMMPRIN as a cancer metastasis marker.

(2) Ongoing experiments investigate the expression of a critical tight junction protein, ZO-1 in prostate tumors with increasing grade. Preliminary staining revealed clear striations of Tight Junctions visualized in epithelial regions that are strongly detected in low-grade tumors and expression is decreased with increasing age of the TRAMP mice. Prostate tumors from 20, 24, 27 and 31-week-old mice are currently being interrogated for tight junction protein expression

that will be correlated with the EMMPRIN expression (an inverse correlation is expected). Please see attachment.

(3) Experiments will be pursuing the consequences of EMMPRIN loss/silencing in prostate cancer cells on the transcriptional regulation of the major players of the process of Epithelial Mesenchymal Translation (EMT). The prostate tumor microenvironment represents a key component of the invasive dynamic of prostate cancer. In reference to this new exciting direction of the work supported by this program, please see as Appendices 1 and two papers published by Dr. Kyprianou's group , an original article and a review article [(Zhu and Kyprianou, The FASEB Journal, 24: 769-777, 2010); (Matuszak and Kyprianou, Expert Rev. Endocrinol. Metabolism, 6: 1-14, 2011)] demonstrating the ability of androgens to induce EMT of prostate cancer epithelial cells.

Comprehensive Presentation of Results:

Development of metastatic prostate cancer is orchestrated by multiple signaling pathways that regulate cell survival, apoptosis, epithelial-mesenchymal transition (EMT), invasion, cytoskeleton remodeling/signaling and angiogenesis. Disruption of the mechanisms underlying these processes and the phenotypic characteristics of their manifestation is critical for metastasis and enhancing therapeutic sensitivity of metastastic tumors to anti-angiogenesis strategies. Targeting the AKT survival pathway and preventing angiogenesis by reducing tumor cell adhesion to the extracellular matrix (ECM), blocking actin organization and filopdia formation and impairing metastasis. Building on the recently published evidence on the functional involvement of EMMPRIN to regulate cytoskeleton reorganization and impact prostate cancer cell invasion (*The Prostate*, 72(1):72-81, 2012), we subsequently pursued the mechanistic dissection of actin remodelling towards promotingprostate tumor progression to metastasis. The actin depolymerizing factor (ADF) cofilin, a small (19kDa) actin binding protein was previously identified by our group to be

an intracellular effector of transforming growth factor beta (TGF-β) in prostate cancer cells. Directing our investigative efforts to identify the consequences of a mutation in cofilin phoshorylation site Serine 3 residue; (S3ACFL) we used the human prostate cancer cell line, that is TGF-β sensitive, androgen-independent PC-3 cells as model. This study has been recently submitted for publication. The results are intriguing as they demonstrated a significant increase in the migration ability for S3ACFL prostate cancer cells compared to the wild type controls. Furthermore there was enhanced adhesion to fibronectin in S3ACFL PC-3 cells, potentially driven by the significantly higher number of filopodia structures in cells harboring the cofilin mutation. TGF-β treatment decreased cell migration, adhesion and filopodia protrusions in the cofilin S3A cells. Of major translational significance that becomes a key accomplishment for this work Is the immunohistochemical analysis of human prostate cancer specimens from primary prostate tumors and lymph node metastatic lesions for expression of cofilin, p-cofilin, palladin and e-cadherin. These proteins are critical players in actin-remodeling through actin cytoskeleton organization and control of epithelial-mesenchymal-transition. Cofilin immunoreactivity correlates with higher tumor grades and moreover there was a significant upregulation of cofilin in metastatic lesions compared to primary tumors. *In vivo* characterization of the metastatic potential of WTCFL and S3ACFL PC-3 cells revealed an increased number of lung metastatic lesions due to cofilin mutation.

The novel findings gathered through this synergy of multidisciplinary approaches, provide evidence to support the ability of cytoskeleton organization regulator proteins, EMMPRIN and cofilin, promote cytoskeletal reorganization of prostate cancer metastasis and establish for the first time the predictive value of both proteins in prostate cancer progression to metastasis.

Key Research Accomplishments: In our collaborative interaction we showed that EMMPRIN loss in human prostate cancer cells, had no significant consequences on prostate cell growth, proliferation or apoptosis. We found,

however, a significant suppression in prostate tumor cell invasion, migration and metastatic ability using in vitro assays. These data are reported in the manuscript to be published in the Prostate (please see as Appendix 1, a copy of the manuscript by Zhu et al, *The Prostate*, 72(1):72-81, 2012) .

My contributions at the translational level have been the determination of the potential predictive value of EMMPRIN in prostate cancer progression, first utilizing the TRAMP mouse model of prostate tumorigenesis and subsequently analyzing a series of human prostate cancer specimens of increasing Gleason grade. The TRAMP mice (C57BL/6J) are transgenic mice that express SV40T/t antigens under the prostate specific rat probasin promoter. TRAMP transgenic males develop prostate adenocarcinoma in a manner resembling the clinical progression of human prostate cancer from intra-epithelial neoplasia to androgen-independent metastatic tumors. Hematoxylin and eosin (H&E)-stained sections of prostate tissues from TRAMP/+/+ male mice were evaluated (by N.K.) to confirm pathological grade. Prostate sections from wild type and the TRAMP tumors of increasing grade and metastatic lesions (5μm), were subjected to immunohistochemical analysis for EMMPRIN expression. As shown in Figure 1 histopathological grading of prostatic tumors revealed that in the majority of 16wk-24wk-old TRAMP mice, prostate adenocarcinoma was evident (16-20weeks),and with increasing age (24 weeks), poorly differentiated tumor foci were detected with focal cribriform lesions protruding into the lumen (grade 3-5), representing tumor progression to advanced disease. A score for each histological grade (H) was determined as the product of intensity and proportion ($H = I \times P$).

Key Research Accomplishments:

This work represented a most creative interaction between two investigators with complementary expertise, prostate tumor biology and proteomics technology with powerful precision towards functional assessment of the biological relevant contributions at both the mechanistic and translational level. Through the proteomic analysis of human prostate cancer cells with different

invasive characteristics and metastatic potential, the award enabled us to a) identify two novel markers of metastatic progression and aggressive phenotype of human prostate cancer; and b) to mechanistically dissect their functional role in the organization of actin cytoskeleton dynamics and remodeling, a fundamentally critical role that heavily impacts the metastastic behavior of prostate cancer cells. The two key proteins that emerged from these synergistic studies, cofilin and EMMPRIN may prove potent and valuable biomarkers of prostate cancer progression in the clinical setting of prostate cancer patients.

Reportable Outcomes : The following publications (two original articles, two chapters and one review article and resulted from the support of the research projects (collabor-ation with Partner-Co-PI, Dr. Zhu through this synergistic idea award).

1. Tang, X., Tang, X., Gal, J., **Kyprianou, N**., Zhu, H. and Tang, G. Detection of microRNAs in prostate cancer cells by microRNA array. Methods in Molecular Biology: MicroRNAs in Development, 732:69-88, 2011.
2. Desiniotis, A. and **Kyprianou, N.** Significance of Talin in Cancer Progression and Metastasis, *International Review of Cell and Molecular Biology,* Elsevier, 2011; Ch. 4, Volume 289, pp.117-147.
3. Zhu, H., Zhao, J., Zhu, B., Collazo, J., Gal, J., Shi, P., Liu, L., Strom, A.L., Lu, X., McCann, R.O., Toborek, M., and **Kyprianou, N**. EMMPRIN Regulates Cytoskeleton Reorganization and Prostate Cancer Cell Invasion, *The Prostate*, 72(1):72-81, 2012. (Appendix 1).
4. Martin, S.K., Vaughan, T.B., Atkinson, T., Zhu, H. and **Kyprianou, N**. Prostate Cancer Biomarker Update*. Oncology Reports,* 28: 409-417*,* 2012. (Review)
5. Colazzo, J., Zhu, B., Horbinski, C. Pu, H. and **Kyprianou, N**. Cofilin, a TGF-β Signaling Effector, Mediates Prostate Tumor Invasion and

Metastasis via Actin Remodelling. *Manuscript submitted for publication*, 2013. (Please see attachment, Appendix 2).

Reportable Outcomes: The expression profile of EMMPRIN expression was assessed during *in vivo* prostate tumorigenesis in the TRAMP model of prostate cancer progression is shown on Figure 1. Our findings reveal strong EMMPRIN immunoreactivity primarily detected among the glandular epithelial cells of prostate tumors from TRAMP mice. Quantitative analysis of the immunoreactivity profile for EMMPRIN revealed that by 24-wks (an age exhibiting highly aggressive prostate tumor phenotype), EMMPRIN expression increased significantly (P=0.001). These results suggest that EMMPRIN may have diagnostic value in prostate cancer detection in advanced disease.

Figure 1

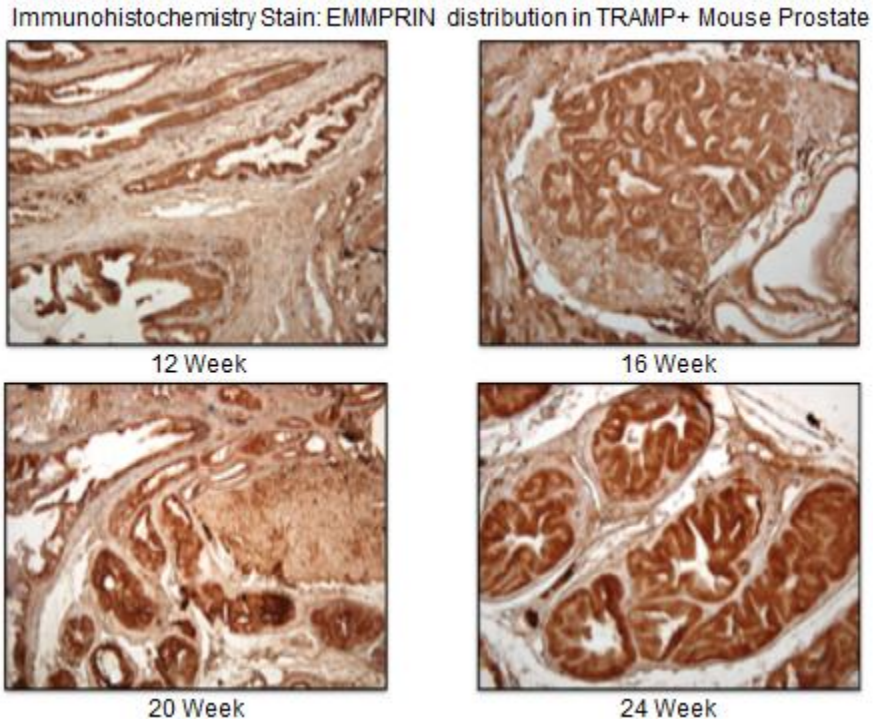
Immunohistochemistry Stain: EMMPRIN distribution in TRAMP+ Mouse Prostate
12 Week
16 Week
20 Week
24 Week

Appendix 1

EMMPRIN Regulates Cytoskeleton Reorganization and Cell Adhesion in Prostate Cancer

Haining Zhu[1,2], Jun Zhao[1], Beibei Zhu[3], Joanne Collazo[2,3], Jozsef Gal[1], Ping Shi[1], Li Liu[1], Anna-Lena Ström[1], Xiaoning Lu[1], Richard O. McCann [1,+], Michal Toborek[4], and Natasha Kyprianou [1, 2,3*]

[1]Department of Molecular and Cellular Biochemistry, [2]Department of Toxicology, [3]Division of Urology, Department of Surgery, and [4]Department Neurosurgery, College of Medicine, University of Kentucky, Lexington, KY 40536

[+] Current address: Mercer University School of Medicine, Division of Basic Medical Sciences, 1550 College Street, Macon, GA 31207

[*] Address correspondence to:
Dr. Natasha Kyprianou
Division of Urology
Combs Res. Bldg. Rm 306
University of Kentucky Medical Center
Lexington, KY 40536
Email: nkypr2@uky.edu
Tel. 1-859-323-9812
Fax: 1-859-323-1944

Running title: Role of EMMPRIN in prostate cancer progression

Abbreviations: EMMPRIN, extracellular matrix metalloprotease inducer; shRNA, short hairpin RNA; PBS, phosphate buffer saline; MMP, matrix metalloprotease; ECM, extracellular matrix; BPH, benign prostatic hyperplasia; VEGF, vascular endothelial growth factor; TUNEL, terminal UTP end-labeling; SDS-PAGE, sodium-dodecyl-sulphate polyacrylamide gel electrophoresis; MTT, 3-(4,5-dimethylthiazol-2-yl)-2,5-diphenyltetrazolium salt.

ABSTRACT

Background. Proteins on cell surface play important roles during cancer progression and metastasis via their ability to mediate cell-to-cell interactions and navigate the communication between cells and the microenvironment.

Methods. In this study a targeted proteomic analysis was conducted to identify the differential expression of cell surface proteins in human benign (BPH-1) vs. malignant (LNCaP and PC-3) prostate epithelial cells. We identified EMMPRIN (extracellular matrix metalloproteinase inducer) as a key candidate and shRNA functional approaches were subsequently applied to determine the role of EMMPRIN in prostate cancer cell adhesion, migration, invasion as well as cytoskeleton organization.

Results. EMMPRIN was found to be highly expressed on the surface of prostate cancer cells compared to BPH-1 cells, consistent with a correlation between elevated EMMPRIN and metastasis found in other tumors. No significant changes in cell proliferation, cell cycle progression or apoptosis were detected in EMMPRIN knockdown cells compared to the scramble controls. Furthermore, EMMPRIN silencing markedly decreased the ability of PC-3 cells to form filopodia, a critical feature of invasive behavior, while it increased expression of cell-cell adhesion and gap junction proteins.

Conclusions: Our results suggest that EMMPRIN regulates cell adhesion, invasion and cytoskeleton reorganization in prostate cancer cells. This study identifies a new function for EMMPRIN as a contributor to prostate cancer cell-

cell communication and cytoskeleton changes towards metastatic spread, and suggests its potential value as a marker of prostate cancer progression to metastasis.

Key words: **Prostate Cancer, EMMPRIN, Cytoskeleton, shRNA, Filopodia**

INTRODUCTION

Metastatic prostate cancer is a major contributor to cancer related mortality in men. Normal prostate epithelial cell homeostasis is maintained by a dynamic balance between cell proliferation and apoptosis. Normal cells undergo anoikis (a unique mode of apoptosis) upon detachment from extracellular matrix (ECM). Cancer cells however develop mechanisms to evade anoikis and acquire the ability to detach and migrate into new sites that provide a nurturing microenvironment for continued growth (1). During the metastatic spread of primary tumor cells, proteins on cell surface are critical in mediating cell to cell and cell to environment communication.

EMMPRIN is a cell surface glycoprotein of IgG superfamily encoded by a gene localized to 19p13.3 (2, 3). EMMPRIN is an integral membrane protein, but may be released as a soluble protein by vesicle shedding (4, 5). It initiates the function through homophilic interactions between EMMPRIN molecules on neighboring cells (4, 5). EMMPRIN is expressed in numerous normal and malignant cells and mediates diverse processes such as angiogenesis, neuronal signaling, cell differentiation, wound healing, and embryo implantation (6). Mice lacking EMMPRIN demonstrate various defects, including low embryonic survival, infertility, deficiencies in learning and memory, abnormality in odor reception, retinal dysfunction, and mixed lymphocyte reaction (6-10). Elevated expression of EMMPRIN is found in several human cancers and correlates with the metastatic potential of tumor cells, specifically in breast and

ovarian cancer epithelial cells during progression to metastasis (11-14). In the context of the tumor microenvironment, EMMPRIN induces matrix metalloproteinase (MMP) production in stromal fibroblasts and endothelial cells as well as in tumor cells (11-13, 15-17). Elevated MMPs result in ECM degradation and subsequent detachment and metastasis of cancer cells. In addition, EMMPRIN can promote tumor cell invasion via activation of urokinase-type plasminogen activator (18), stimulate tumor angiogenesis by elevating vascular endothelial cell growth factor (VEGF) through Akt signaling (19), and causes multi-drug resistance in tumor cells via hyaluronan-mediated up-regulation and ErbB2 signaling activation (20). EMMPRIN is implicated in metastasis via its ability to confer resistance of breast cancer cells to anoikis by inhibiting BIM (21), and its association with lipid raft or caveolae via interactions with key membrane proteins, including caveolin-1, monocarboxylate transporters, annexin II, (22) and integrins α2β1, α3β1, α6β1 (23), all critical in the spatial distribution and activity of EMMPRIN.

Previous studies suggested that EMMPRIN expression is associated with prostate cancer progression (24, 25), and loss of EMMPRIN reduces the invasion potential of human prostate cancer cells (26). This evidence however has been correlative and little is known about the mechanistic significance of EMMPRIN in prostate cancer progression and metastasis beyond its ability to induce MMPs. In this study we profiled the EMMPRIN expression pattern in human prostate cell lines of benign and metastatic origin and characterized the function of EMMPRIN in tumor cell aggressive behavior. EMMPRIN

suppression led to a significant decrease in prostate cancer cell attachment to the ECM, migration and invasion, as well as filopodia formation while it enhanced cell-cell interactions. The results provide a new insight into the ability of EMMPRIN to regulate prostate cancer cell adhesion, invasion and cytoskeleton organization.

MATERIALS AND METHODS

Cell Lines. The HEK293 and the human prostate cancer cell lines PC-3, DU-145 and LNCaP, were obtained from the American Type Culture Collection (Manassas, VA). The nontumorigenic benign human prostatic epithelial cells BPH-1, (derived from human prostate epithelium of benign pathology) was generously provided by Dr. Simon W. Hayward (Department of Urological Surgery, Vanderbilt University Medical Center). Cells are maintained in RPMI-1640 medium (Gibco^{TM}, Grand Island, NY), supplemented with 10% fetal calf serum (CSS), 100U penicillin and 100-mg/ml streptomycin, at 5% CO_2 incubator at 37 ºC.

Western Blot Analysis. Confluent cell cultures (80%) were washed with PBS, scraped, and cell pellets were harvested. Cells were disrupted with RIPA buffer (50 mM Tris-HCl, pH7.4, 1% NP40, 0.25% Na-deoxycholate, 150 mM NaCl, 1 mM EDTA, 1 mM PMSF, 1 mg/mL each of aprotinin, leupeptin, pepstatin, and 1 mM Na_3VO_4). Cell lysates were centrifuged at 5,000xg (15mins), resolved by SDS-PAGE, and transferred to Immobilon-P membranes (Millipore, Bedford, Mass.). Upon incubation with the primary and secondary antibodies, immunoreactive bands were detected using a chemiluminescent approach with the ECL kit (Pierce, Rockford, IL). Membrane fractions were

prepared using the protein isolation kit (Pierce). Monoclonal antibodies against EMMPRIN, ZO-2, actin and tubulin were purchased from Santa Cruz Biotech (Santa Cruz, CA). Monoclonal antibodies against ZO-1 and AF6 were obtained from Invitrogen Zymed (San Francisco, CA) and BD Transduction (Lexington, KY), respectively.

RT-PCR analysis. Total RNA was extracted from cells using an RNAeasy kit (Qiagen, Valencia, CA). RNA samples (0.25µg) were subjected to reverse transcription (RT) PCR reaction in a 20-µl volume with poly-oligoT primer. The resulting cDNA was subjected to PCR using EMMPRIN specific primers. The first set of primers started with exon 1 and ended at exon 11: EF2 (5'-ATG GCG GCT GCG CTG TTC GTG-3') and ER11 (5'-GGA GCA GGG AGC GTC CTC GGG-3'). The second set of primers started with exon 2 and ended at exon 11: EF1 (5'-ATG AAG CAG TCG GAC GCG TCT C-3') and ER11. GAPDH primers (5'-CAG CAA TGC ATC CTG CAC-3' and 5'-GAG TTG CTG TTG AAG TCA CAG G-3') were used as control in the same PCR reactions. Thirty cycles of PCR reactions were performed and each cycle included 45 sec, 94°C; 45sec, 55°C; and 45sec, 72°C. The PCR products were analyzed on a 1.2% agarose gel. Amplicons are purified, cloned and sequenced by IDT (Coralville, IA).

shRNA Plasmid Construction and Transfection. Short hairpin RNA (shRNA) interference oligos, were designed using OligoEngine software (Seattle, WA) to specifically target EMMPRIN (NM_198589). Three oligos that target EMMPRIN (variant 2 mRNA) at nucleotides 98-116

(TGGCTCCAAGATACTCCTC), 277-295 (CCATGGGCACGGCCAACAT) and 776-794 (AGGCAAGAACGTCCGCCAG), are named as 98i, 277i and 776i, respectively. A scramble shRNA (TTCTCCGAACGTGTCACGT) was used as control. The oligos are cloned to pSUPER (neo + GFP) plasmid from OligoEngine according to the manufacturer's instruction. Plasmids were amplified in DH5α cell and confirmed by sequencing.

Subconfluent cell populations were used for transfection using the FuGENE system (Roche, Indianapolis, IN). Briefly, the plasmid and Fugene reagent were combined and incubated for 20-30mins at room temperature. After transfection (36hrs), cells were subjected to cell sorting based on GFP expression and GFP positive cells were subsequently subjected to Western blotting. Stable tansfectants were cloned under Geneticin selection (Invitrogen) (300μg/ml), the generated clones were maintained in RPMI 1640 medium (150μg/ml Geneticin).

Cell Viability Assay. The MTT assay (based on the ability of viable mitochondria to convert MTT, a soluble tetrazolium salt, into an insoluble formazan precipitate) was used to assess cell viability. Cells were seeded into 96-well plates (2,500 cells/well) and incubated in growth medium (18-24hrs). After incubation with the MTT solution for 4 hrs, absorbance was read at A_{570} and the colorimetric reaction product was quantitated spectrophotometrically (BioTek, PowerWave XS, Winooski, VT).

Evaluation of Cell Cycle and Apoptosis. BrdU/PI (Bromodeoxy uridine and propidium iodide) method was used for the analysis of cell cycle

progression and apoptosis. Cells ($1x10^6$/ml) were incubated with BrdU (20mM) (60min at 37°C), suspended in PBS, and fixed with ice-cold 95% (v/v) ethanol. Fixed cells were subsequently permeabilized using pepsin (0.04% w/v, 0.4mg/mL in 0.1N HCl). BrdU was probed with FITC labeled anti-BrdU (BD, San Jose, CA). Apoptosis among the different cell populations was evaluated using the terminal UTP end-labeling (TUNEL) technique. (Leica, Germany).

Cell Adhesion Assay. The ability of cells to attach to key ECM components, (fibronectin and laminin) was tested using fibronectin or laminin-coated 6-well multiwell plates (BD Bioscience). Prostate cancer epithelial cells were plated (10^5/well), and incubated at 37°C for 30mins, prior to fixing with methanol, and washed with PBS. Cells were counted from three random fields/well.

Evaluation of Cell Migration and Invasion. Confluent monolayer cells were wounded by scraping. Cultures were washed twice with medium, and then incubated at 37 °C for 16hrs to allow migration toward the gap. The number of migrating cells was determined under the microscope. The invasion potential of prostate cancer cells was assessed using Biocoat Matrigel invasion chambers (Becton Dickinson). Briefly, cells ($5x10^4$) resuspended in RPMI1640-based medium were added (250µl) into the invasion chambers and chambers were subsequently inserted into 24-well plates. Stained cells were photographed and counted.

Confocal Microscopy. Cells were plated on fibronectin-coated glass coverslips and fixed with 4% paraformaldehyde. Cells were permeablized in

0.1% (v/v) Triton-X 100 and were subsequently stained with rhodamine-phalloidin (Jackson ImmunoResearch, West Grove, PA). After rinsing with PBS (3x), slides were mounted with Vectorshield (Vector Lab, Burlingame, CA). Slides were examined under a laser-scanning confocal microscope (Leica Lasertechnik, Heidelberg, Germany).

Cell Aggregation Assay. Cells aggregation assay was performed as previously described (27). Briefly, cells were suspended into single cells and dissociated cells were allowed to associate in medium (1hr) in 5% CO_2 at 37ºC, with gentle rotation of the plates. The number of cell aggregates in the parental control PC-3 and EMMPRIN shRNA transfectant cells was counted.

Statistical Analysis. Data are expressed as Mean ± SD. Mann-Whitney and Student's t tests were used to comparatively analyze the differences between groups in the various experiments.

RESULTS

EMMPRIN Expression in Human Prostate Cancer Cell Lines

Targeted proteomic analysis comparing the cell surface proteomes of BPH-1 (immortalized benign prostate hyperplasia cell line) and LNCaP and PC-3 (human prostate cancer cell lines derived from metastatic lesions) revealed the differential expression of EMMPRIN. EMMPRIN was found to be highly expressed on the cell surface of prostate cancer epithelial cells but not the benign prostate cells. Western blot analysis was subsequently conducted to

validate the proteomics screening data and the results are shown in Figure 1. Using total cell lysates (Fig. 1, panel A), EMMPRIN showed a broad range molecular shift corresponding to different degrees of glycosylation as previously shown in breast cancer cells (11-13). Malignant prostate cells, PC-3 and LNCaP appeared to have more highly glycosylated EMMPRIN than BPH-1 while the total protein levels were similar in all three cell lines. Glycosylation of EMMPRIN contributes to its membrane localization. Thus plasma membrane fractions were isolated from all prostate cell lines and subjected to Western blotting. As shown in Figure 1B, EMMPRIN levels in the plasma membrane fractions of LNCaP and PC-3 cells were significantly higher than in BPH-1 cells. These results are consistent with the cell surface proteome studies, implicating higher EMMPRIN translocation to the plasma membrane in prostate cancer cells than in benign cells. The molecular mechanism of membrane targeting and translocation is beyond the scope of this article and is currently being pursued in a parallel study.

The alternative splicing isoforms of EMMPRIN in the prostate cell lines were also determined. Four splicing isoforms of EMMPRIN have been deposited in the NCBI database and most studies focus on variant 2 that harbor two Ig domains. Two sets of primers were designed for RT-PCR: one starting at exon 1 and ending at exon 11, and the other one starting at exon 2 and ending at exon 11. The RT-PCR products were analyzed by agarose electrophoresis and the results are shown in Figure 1 (Panel C). The RT-PCR products were cloned and subjected to DNA sequencing. The sequencing results

demonstrated that there are three different splicing variants existed in human prostate cells: variant 2 (band 3, 828bp), variant 4 (band 1, 634bp) and variant 3 (band 2, 793bp). Other bands indicated by filled triangles were non-specific RT-PCR products. Variant 2 appeared to be the major transcript in human prostate cells and there were no evident differences in the splicing isoforms among the different cell lines

EMMPRIN Silencing in PC-3 Prostate Cancer Cells

The functional significance of EMMPRIN in prostate cancer progression remains unknown. Thus we examined whether high levels of EMMPRIN in PC-3 cells, functionally contribute to the aggressive behavior of metastatic prostate cancer cells. Since PC-3 exhibit high endogenous EMMPRIN expression, we used the RNA interference approach to silence EMMPRIN in these cells. Three pairs of oligos targeting to EMMPRIN exon 5, 6 and 11 were designed and successfully cloned into pSUPER plasmid (containing GFP marker). Due to the low transfection efficiency in PC-3 cells (about 30% using FuGENE), cells with the GFP marker were sorted at 36hrs after transfection and were subjected to Western blot analysis. The results shown in Figure 2A indicate that EMMPRIN protein levels are significantly reduced by all three shRNA species. Stable clones in which EMMPRIN was silenced under G418 selection, had lower EMMPRIN levels compared to scramble controls (Fig. 2, panels A and B).The shRNA 277 clone, in which the middle region of EMMPRIN gene was targeted, had less of an effect in reducing EMMPRIN expression.

Effect of EMMPRIN Loss on Prostate Cancer Cell Proliferation and Apoptosis

To determine the role of EMMPRIN on prostate cancer cell growth, we initially examined the consequences of EMMPRIN silencing on prostate cancer cell proliferation, cell cycle and apoptosis. Interestingly, down-regulation of EMMPRIN resulted only in a modest inhibitory effect on prostate cancer cell growth (Supplementary Figure S1, panel A). Cell cycle analysis demonstrated no significant effect on cell cycle progression in shRNA EMMPRIN PC-3 transfectants (Fig. S1, panel B). Evaluation of apoptosis based on the TUNNEL assay revealed that loss of EMMPRIN had no significant consequences on the rate of cell death among these cell populations (Fig. S1, panel C). Thus EMMPRIN is not involved in the control of prostate cancer cell growth or apoptosis.

EMMPRIN Loss Decreases Prostate Cancer Cell Adhesion, Migration and Invasion

Many cell surface proteins are involved in cell adhesion and EMMPRIN can be a potential partner with such adhesion molecules. To determine the functional contribution of EMMPRIN to prostate cancer cell adhesion to the ECM, we examined attachment ability of EMMPRIN silenced PC-3 transfectants to key components of the ECM, fibronectin and laminin. As shown on Figure 3 (Panel A), there was a 40% decrease in the number of cells

attached to fibronectin for the EMMPRIN knockdown cells compared to the scramble control cells. A similar magnitude of suppression of cell adhesion to laminin was observed in the EMMPRIN shRNA stable clones compared to scramble control cells (Fig. 3, panel B) or PC-3 parental cells (approximately 30-50% suppression). We subsequently examined the consequences of EMMPRIN loss on prostate cancer cell migration. EMMPRIN silencing yielded a significant reduction in cell migration ability in all three shRNA prostate cancer cell lines (Fig. 3, panel B), with the s277i clone exhibiting the most significant suppression. In addition, we examined the impact of EMMPRIN loss on the invasion ability of PC-3 cells. Figure 3 (Panel C), shows a significant decrease in cell invasion observed in EMMPRIN shRNA transfected cells compared to control cells. Thus loss of EMMPRIN significantly decreased the adhesion, migration and invasion abilities of metastatic prostate cancer cells.

EMMPRIN Enhanced Filopodia Formation in Prostate Cancer Cells

To determine whether EMMPRIN promotes cell migration by facilitating cytoskeleton reorganization, we examined the ability of EMMPRIN shRNA PC-3 cells, to form filopodia. Cells attached to fibronectin-coated cover-slips were subjected to immunefluorescence analysis for vinculin and F-actin presence and localization. The image on Figure 4 (Panel A), indicates that EMMPRIN silencing inhibited prostate cancer cell spreading on fibronectin, while a stronger F-actin staining was detected forming a stress fiber but without typical focal adhesion complex (Fig.4, panel A). Confocal microscopy revealed a

significant suppression of filopodia formation as a consequence of EMMPRIN loss. An approximate 50% reduction in the number of filopodia is detected in EMMPRIN knockout cells compared to control cells (Fig. 4, panel B). In addition, EMMPRIN silencing also led to a decrease in the strength of the filopodia. Immunofluorescence analysis (Fig. 4, panel A) revealed considerably larger filopodia in control cells compared to limited and small filopodia observed among EMMPRIN knockdown PC-3 prostate cancer cells.

Effect of EMMPRIN Knockdown on Cell Aggregation and Tight Junction Proteins

We subsequently examined the effect of EMMPRIN on the dissociation/detachment of cancer cells. A cell aggregation assay was conducted in the PC-3 control and EMMPRIN shRNA PC-3 prostate cancer cells. As shown in Figure 5 (Panel A), there was increased cell aggregation in EMMPRIN silenced PC-3 cells. Subsequent experiments determined the effect of EMMPRIN silencing on the expression of tight junction proteins. The levels of plasma membrane proteins JAM-A and JAM-B were unchanged in the EMMPRIN knockdown clones (Fig. 5, panel B). A significant increase however in the levels of tight junction associated proteins ZO-1, ZO-2, AF6 and β-catenin was detected consequential to EMMPRIN loss. These data imply that EMMPRIN may impair cell-cell interactions by facilitating the dissociation/detachment of tumor epithelial cells from each other.

DISCUSSION

To determine the cell surface protein differences between malignant and benign prostate cells and their significance in prostate cancer metastasis, we performed mass spectrometry analysis to profile the expression of cell surface proteins in human prostate cancer cells derived from metastatic lesions and benign prostate epithelial cells. One of the proteins highly expressed on the cell surface of metastatic prostate cancer cells, but not benign cells, was identified to be extracellular matrix metalloproteinase inducer (EMMPRIN, also known as basigin, CD147, OX47 or 5A11). EMMPRIN has been previously shown to be involved in cancer development via its ability to stimulate MMP production and consequently control extracellular matrix remodeling and anchor independent growth (28). In addition, EMMPRIN has been shown to regulate angiogenesis by engaging the AKT-PIK3 pathway (19), and to up-regulate urokinase-type plasminogen activator (18). EMMPRIN can also interact with key adhesion proteins such as integrins (23), implicating its role in cancer cell migration and invasion. The present study provides the first evidence on the functional consequences of EMMPRIN loss on prostate cancer cell growth, proliferation, apoptosis and cell adhesion (Fig 3). We observed that down-regulation of EMMPRIN led to a significant suppression of prostate cancer attachment to fibronectin, a major ECM component (Fig. 4, panel A). Thus a defect in the cytoskeleton organization can be induced by functional loss of EMMPRIN. Furthermore down regulation of EMMPRIN protein led to decreased prostate

cancer cell migration. Considering the evidence that cell migration is independent of MMPs and that MMP and EMMPRIN knockout mice (29) have different phenotypes, it is reasonable to postulate that these two proteins may operate in independent pathways functionally converging downstream. EMMPRIN may be engaged in distinct signaling pathways, directly promoting the invasive behavior of prostate cancer cells towards metastasis. This notion gains support from evidence indicating lack of correlation between EMMPRIN expression and MMP activity during adult mouse mammary gland development (30). Moreover, EMMPRIN has been shown to directly promote insoluble fibronectin assembly (21).

In this study, EMMPRIN loss significantly reduced prostate cancer cell filopodia formation on a fibronectin substratum. This defective filopodia formation implies disruption of cytoskeleton organization and actin signaling in cells lacking EMMPRIN. These observations are consistent with reports suggesting that EMMPRIN (D-basigin in Drosophila) tightly regulates cytoskeleton rearrangement in *Drosophila melanogaster* (23). Based on the present results and the existing evidence, we propose that EMMPRIN promotes tumor cell metastasis in an MMP-dependent and -independent pathway (Fig. 5, panel C). One must also consider that EMMPRIN has been associated with prominent membrane proteins caveolin-1 and vimentin, implicating its involvement in lipid raft and control of membrane dynamics. Here we show for the first time that silencing EMMPRIN resulted in enhanced cell aggregation (Fig. 5, panel A) and increased the protein expression for several tight-junctions

mediators including ZO-1, ZO-2, AF-6 and β-catenin (Fig. 5, panel B). Considering the reported relationship between tight junction proteins and cytoskeletal changes associated with cell aggregation (27, 31) our findings provide new insights into the ability of elevated EMMPRIN to navigate tight junctions and cell-cell adhesion within the tumor microenvironment. The mechanistic scenario discussed above can lead to enhanced prostate cancer invasiveness by EMMPRIN overexpression. Significantly enough, our group recently demonstrated that talin1, an actin-binding protein that links integrins to actin cytoskeleton in focal adhesion complexes, correlated with prostate cancer progression to metastasis (32). Mechanistically, talin1 binding to β integrin recruits the focal adhesion partners ILK, FAK and SRC, and activates downstream signals, PI3K/Akt and Erk; activation of this signaling promotes cell survival, migration and invasion and resistance to anoikis. EMMPRIN may serve as an upstream partner for talin, facilitating its role in anoikis resistance and actin cytoskeleton remodeling, and consequently promoting metastatic spread.

Mammalian cells ubiquitously adopt a variant splicing strategy to cope with multiple functions and their requirement by diverse physiological processes. At least two different variants of EMMPRIN have been reported. Variant 2 is a ubiquitous expression protein as previously reported and a larger variant 1 is expressed in retinal epithelial cells in a tissue specific fashion. In this study, we identified three distinct EMMPRIN splicing variants: variant 2, 3 and 4 (Fig. 1, panel C). The latter two variants are distinct from the commonly

found variant 2. Significantly enough these two variants lack exon 2 where glycosylation occurs (3). Moreover, variant 4 lacks exon 5, where another glycosylation site is also located. The dynamics of the ratio of different isoforms and the mechanisms via which the different splicing variants are engaged to navigate EMMPRIN expression and activity to meet the physiological demands of both ECM remodeling and cancer cell motility are currently being pursued.

The present results are of translational significance as functional exploitation of EMMPRIN in prostate cancer metastasis may lead to new approaches for impairing the metastatic process by a) reversing the ability of tumor cells to resist anoikis (thus enhancing their sensitivity to anoikis-inducing agents); and b) interfering with the tumor cell migration and adhesion to secondary sites. Ongoing studies focus on immunoprofiling EMMPRIN expression in human prostate specimens from patients with primary and metastatic tumors to determine the significance of EMMPRIN as a marker of progression to advanced castration-resistant disease.

In summary, our findings demonstrate that EMMPRIN loss has a major impact on cell membrane re-organization and spatial disruptions that significantly affect prostate tumor cell adhesion, migration and invasion. The present work provides new insights into the function of EMMPRIN as a contributor to prostate cancer cell metastatic behavior and its potential value as a therapeutic target during tumor progression.

ACKNOWDGEMENTS

This work was supported by a Department of Defense Synergistic Idea Development Award W81XWH-08-1-0430 (to H.Z) and W81XWH-08-1-0431 (to N.K.), an NIH/NCRR COBRE grant 1P20RR020171 (to H.Z and N.K.), and an NIH/NIDDK grant R01DK053525 (to N.K). The Proteomics Core supported by COBRE grant 1P20RR020171 is also acknowledged. The authors are grateful to Dr. Steven Schwarze (Department of Biochemistry) for useful discussions and Lorie Howard for her expert assistance in the submission of the manuscript.

REFERENCES

1. Rennebeck G, Martelli M, Kyprianou N. Anoikis and survival connections in the tumor microenvironment: is there a role in prostate cancer metastasis? Cancer Res 2005; 65:11230-5.
2. Biswas C, Zhang Y, DeCastro R, Guo H, Nakamura T, Kataoka H, et al. The human tumor cell-derived collagenase stimulatory factor (renamed EMMPRIN) is a member of the immunoglobulin superfamily. Cancer Res 1995; 55:434-9.
3. Guo H, Majmudar G, Jensen TC, Biswas C, Toole BP, Gordon MK. Characterization of the gene for human EMMPRIN, a tumor cell surface inducer of matrix metalloproteinases. Gene 1998; 220:99-108.
4. Sidhu SS, Mengistab AT, Tauscher AN, LaVail J, Basbaum C. The microvesicle as a vehicle for EMMPRIN in tumor-stromal interactions. Oncogene 2004; 23:956-63.
5. Yan L, Zucker S, Toole BP. Roles of the multifunctional glycoprotein, emmprin (basigin; CD147), in tumour progression. Thromb Haemost 2005; 93:199-204.
6. Muramatsu T, Miyauchi T. Basigin (CD147): a multifunctional transmembrane protein involved in reproduction, neural function, inflammation and tumor invasion. Histol Histopathol 2003; 18:981-7.
7. Igakura T, Kadomatsu K, Taguchi O, Muramatsu H, Kaname T, Miyauchi T, et al. Roles of basigin, a member of the immunoglobulin superfamily, in behavior as to an irritating odor, lymphocyte response, and blood-brain barrier. Biochem Biophys Res Commun 1996; 224:33-6.
8. Naruhashi K, Kadomatsu K, Igakura T, Fan QW, Kuno N, Muramatsu H, et al. Abnormalities of sensory and memory functions in mice lacking Bsg gene. Biochem Biophys Res Commun 1997; 236:733-7.
9. Hori K, Katayama N, Kachi S, Kondo M, Kadomatsu K, Usukura J, et al. Retinal dysfunction in basigin deficiency. Invest Ophthalmol Vis Sci 2000; 41:3128-33.
10. Kuno N, Kadomatsu K, Fan QW, Hagihara M, Senda T, Mizutani S, et al. Female sterility in mice lacking the basigin gene, which encodes a transmembrane glycoprotein belonging to the immunoglobulin superfamily. FEBS Lett 1998; 425:191-4.
11. Caudroy S, Polette M, Tournier JM, Burlet H, Toole B, Zucker S, et al. Expression of the extracellular matrix metalloproteinase inducer (EMMPRIN) and the matrix metalloproteinase-2 in bronchopulmonary and breast lesions. J Histochem Cytochem 1999; 47:1575-80.
12. Caudroy S, Polette M, Nawrocki-Raby B, Cao J, Toole BP, Zucker S, et al. EMMPRIN-mediated MMP regulation in tumor and endothelial cells. Clin Exp Metastasis 2002; 19:697-702.
13. Taylor PM, Woodfield RJ, Hodgkin MN, Pettitt TR, Martin A, Kerr DJ, et al. Breast cancer cell-derived EMMPRIN stimulates fibroblast MMP2 release

through a phospholipase A(2) and 5-lipoxygenase catalyzed pathway. Oncogene 2002; 21:5765-72.
14. Davidson B, Goldberg I, Berner A, Kristensen GB, Reich R. EMMPRIN (extracellular matrix metalloproteinase inducer) is a novel marker of poor outcome in serous ovarian carcinoma. Clin Exp Metastasis 2003; 20:161-9.
15. Toole BP. Emmprin (CD147), a cell surface regulator of matrix metalloproteinase production and function. Curr Top Dev Biol 2003; 54:371-89.
16. Jia L, Cao J, Wei W, Wang S, Zuo Y, Zhang J. CD147 depletion down-regulates matrix metalloproteinase-11, vascular endothelial growth factor-A expression and the lymphatic metastasis potential of murine hepatocarcinoma Hca-F cells. Int J Biochem Cell Biol 2007; 39:2135-42.
17. Yang JM, Xu Z, Wu H, Zhu H, Wu X, Hait WN. Overexpression of extracellular matrix metalloproteinase inducer in multidrug resistant cancer cells. Mol Cancer Res 2003; 1:420-7.
18. Quemener C, Gabison EE, Naimi B, Lescaille G, Bougatef F, Podgorniak MP, et al. Extracellular matrix metalloproteinase inducer up-regulates the urokinase-type plasminogen activator system promoting tumor cell invasion. Cancer Res 2007; 67:9-15.
19. Tang Y, Nakada MT, Rafferty P, Laraio J, McCabe FL, Millar H, et al. Regulation of vascular endothelial growth factor expression by EMMPRIN via the PI3K-Akt signaling pathway. Mol Cancer Res 2006; 4:371-7.
20. Ghatak S, Misra S, Toole BP. Hyaluronan constitutively regulates ErbB2 phosphorylation and signaling complex formation in carcinoma cells. J Biol Chem 2005; 280:8875-83.
21. Yang JM, O'Neill P, Jin W, Foty R, Medina DJ, Xu Z, et al. Extracellular matrix metalloproteinase inducer (CD147) confers resistance of breast cancer cells to Anoikis through inhibition of Bim. J Biol Chem 2006; 281:9719-27.
22. Gupta N, Wollscheid B, Watts JD, Scheer B, Aebersold R, DeFranco AL. Quantitative proteomic analysis of B cell lipid rafts reveals that ezrin regulates antigen receptor-mediated lipid raft dynamics. Nat Immunol 2006; 7:625-33.
23. Curtin KD, Meinertzhagen IA, Wyman RJ. Basigin (EMMPRIN/CD147) interacts with integrin to affect cellular architecture. J Cell Sci 2005; 118:2649-60.
24. Han ZD, Bi XC, Qin WJ, He HC, Dai QS, Zou J, et al. CD147 Expression Indicates Unfavourable Prognosis in Prostate Cancer. Pathol Oncol Res 2009; 15(3):369-74.
25. Zhong WD, Han ZD, He HC, Bi XC, Dai QS, Zhu G, et al. CD147, MMP-1, MMP-2 and MMP-9 protein expression as significant prognostic factors in human prostate cancer. Oncology 2008; 75:230-6.
26. Wang L, Wu G, Yu L, Yuan J, Fang F, Zhai Z, et al. Inhibition of CD147 expression reduces tumor cell invasion in human prostate cancer cell line via RNA interference. Cancer Biol Ther 2006; 5:608-14.
27. Takai E, Tan X, Tamori Y, Hirota M, Egami H, Ogawa M. Correlation of translocation of tight junction protein Zonula occludens-1 and activation of epidermal growth factor receptor in the regulation of invasion of pancreatic cancer cells. Int J Oncol 2005; 27:645-51.

28. Marieb EA, Zoltan-Jones A, Li R, Misra S, Ghatak S, Cao J, et al. Emmprin Promotes Anchorage-Independent Growth in Human Mammary Carcinoma Cells by Stimulating Hyaluronan Production. Cancer Res 2004; 64:1229-32.
29. Philp NJ, Ochrietor JD, Rudoy C, Muramatsu T, Linser PJ. Loss of MCT1, MCT3, and MCT4 expression in the retinal pigment epithelium and neural retina of the 5A11/basigin-null mouse. Invest Ophthalmol Vis Sci 2003; 44:1305-11.
30. Szymanowska M, Hendry KA, Robinson C, Kolb AF. EMMPRIN (basigin/CD147) expression is not correlated with MMP activity during adult mouse mammary gland development. J Cell Biochem 2009; 106:52-62.
31. Huang W, Eum SY, Andras IE, Hennig B, Toborek M. PPARalpha and PPARgamma attenuate HIV-induced dysregulation of tight junction proteins by modulations of matrix metalloproteinase and proteasome activities. FASEB J 2009; 23:1596-606.
32. Sakamoto, S., McCann, R.O., Dhir, R. and Kyprianou, N. Talin1 Promotes Tumor Invasion and Metastasis via Focal Adhesion Signaling and Anoikis Resistance. Cancer Res., 2010; 70(5):1885-1895.

FIGURE LEGENDS

Figure 1. EMMPRIN expression and alternative splicing in prostate cancer cells. Panel A, EMMPRIN expression levels in total cell lysates of BPH-1, LNCaP and PC-3 cells. Bands of different motilities are likely due to glycosylation. Both LNCaP and PC-3 cell lines exhibited elevated levels of highly glycosylated EMMPRIN compared to BPH-1 cells. Panel B**.** LNCaP and PC-3 prostate cancer cells exhibited a significantly higher amount of membrane anchored EMMPRIN compared to BPH-1 cells. Membrane fractions (30µg protein) were subjected to Western blotting. **(C).** EMMPRIN transcripts were analyzed by RT-PCR and electrophoresis. Splicing variants 2, 3 and 4 were confirmed by DNA sequencing as Band #3, #1 and #2, respectively.

Figure 2. Suppression of EMMPRIN expression in transient and stable shRNA prostate cancer transfected cells. PC-3 cells were transfected with three EMMPRIN shRNA plasmids or scrambled control and subjected to Western blot analysis to establish EMPPPRIN protein expression levels (major band detected at 50 kDa). Panel A, after transient transfection a considerable reduction in EMMPRIN expression was detected in GFP-positive cells transfected with three different shRNA plasmids, while no changes in EMMPRIN levels were observed in the GFP negative control cells. Panel B; stably transfected cells with GFP marker were obtained after selection with G418 (300µg/ml). Substantial reduction in EMMPRIN levels was demonstrated in the individual stable shRNA clones.

Figure 3. Consequences of EMMPRIN silencing on prostate cancer cell adhesion to ECM, migration and invasion. EMMPRIN shRNA transfectant PC-3 cells were seeded on fibronectin-coated (panel A) or laminin (panel B) plates for 30mins and attached cells were fixed and counted. Panel C, Cell migration was assessed by wounding the cell monolayer and determining the number of cells migrating to the wounded area after 24hrs. Panel D, The effect of EMMPRIN silencing on prostate cancer cell invasion was determined using the matrigel assay as described in “Materials and Methods”. The average values from three independent experiments performed in triplicate are shown. Numerical values are expressed as percentage of control Sh scramble cells. Statistical significance is reached at $p<0.01$.

Figure 4. EMMPRIN loss reduces filopodia formation in prostate cancer cells. Panel A. Cells were plated on fibronectin-coated glass coverslips and after spreading (24hrs), they were exposed to F-actin staining, and subsequently visualized under confocal microscopy, Arrow heads indicate individual filopdia. The insert represents a zoom-in of region indicated in doted boxed areas. Panel B, The average number of filopodia in each cell was quantified in scramble control and the three shEMMPRIN clones, 98i, 277i and 776i cells. Filopodia from at least 20 cells were counted and representative average values are shown. Approximately 20 cells/field and 10 random fields were examined for each cell line; error bars indicate average values from these

measurements (mean) ± standard error of mean (SEM) gathered from three independent experiments. Statistical difference is considered significant at $p<0.01$.

Figure 5. Effect of EMMPRIN on cell aggregation and tight junction proteins.

Panel A. Cell aggregation increased with reduced EMMPRIN expression in prostate cancer cell EMMPRIN Sh clones. Panel B, Western blotting indicating expression of gap junction proteins in EMMPRIN silenced PC-3 cells. Panel C, Potential role of EMMPRIN in prostate cancer metastasis. EMMPRIN can stimulate production of MMPs, leading to reduced cell adhesion to ECM. Alternatively, EMMPRIN may directly promote the metastatic potential of prostate cancer cells by enhancing migration and invasion through cytoskeleton reorganization and impairing cell-microenvironment interactions.

Figure 1

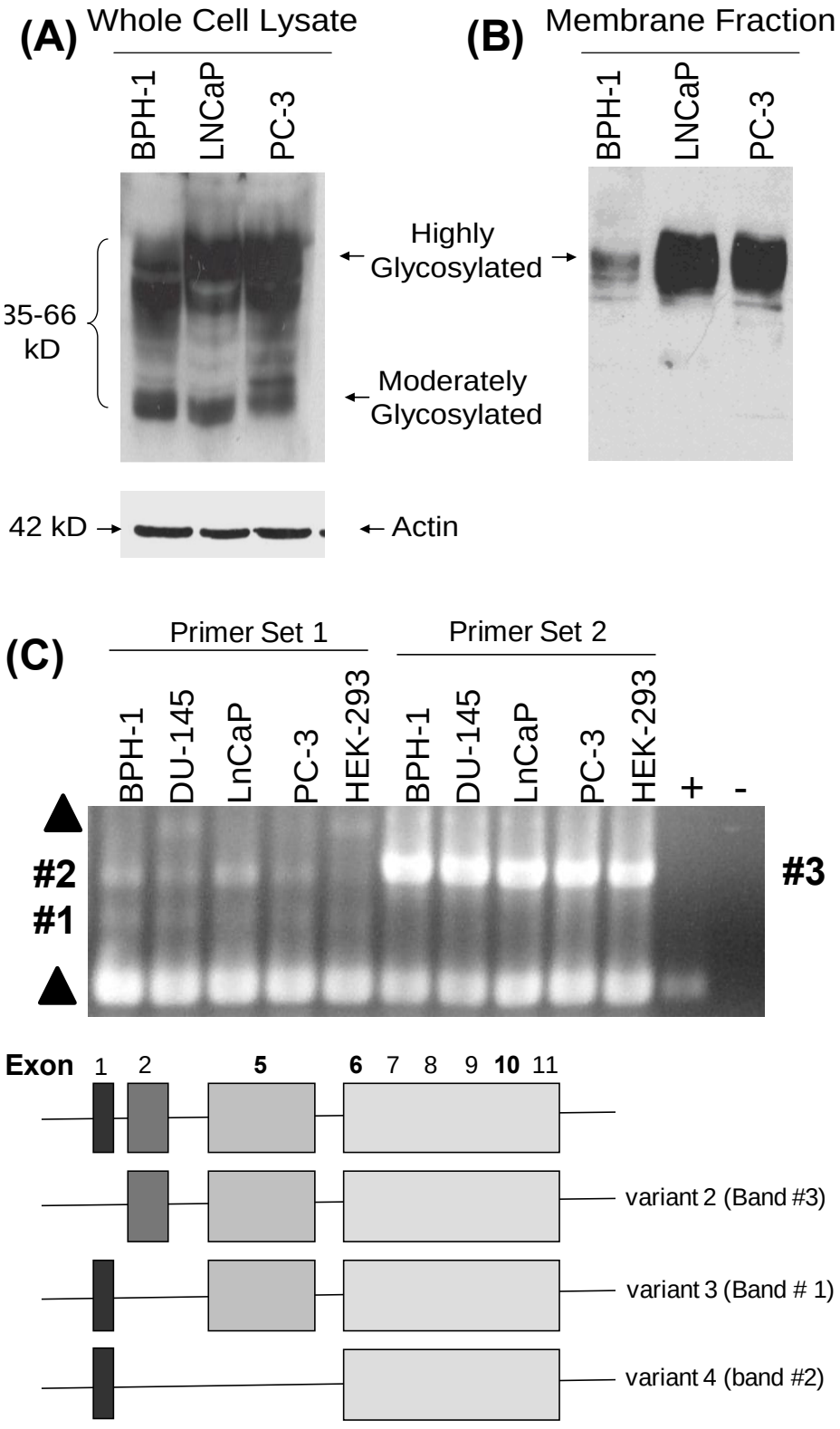
(A)
Whole Cell Lysate
BPH-1
LNCaP
PC-3
35-66 kD
Highly Glycosylated
Moderately Glycosylated
42 kD
Actin
(B)
Membrane Fraction
BPH-1
LNCaP
PC-3
(C)
Primer Set 1
Primer Set 2
BPH-1
DU-145
LnCaP
PC-3
HEK-293
+
-
#2
#1
#3
Exon 1 2 5 6 7 8 9 10 11
variant 2 (Band #3)
variant 3 (Band # 1)
variant 4 (band #2)

Figure 2

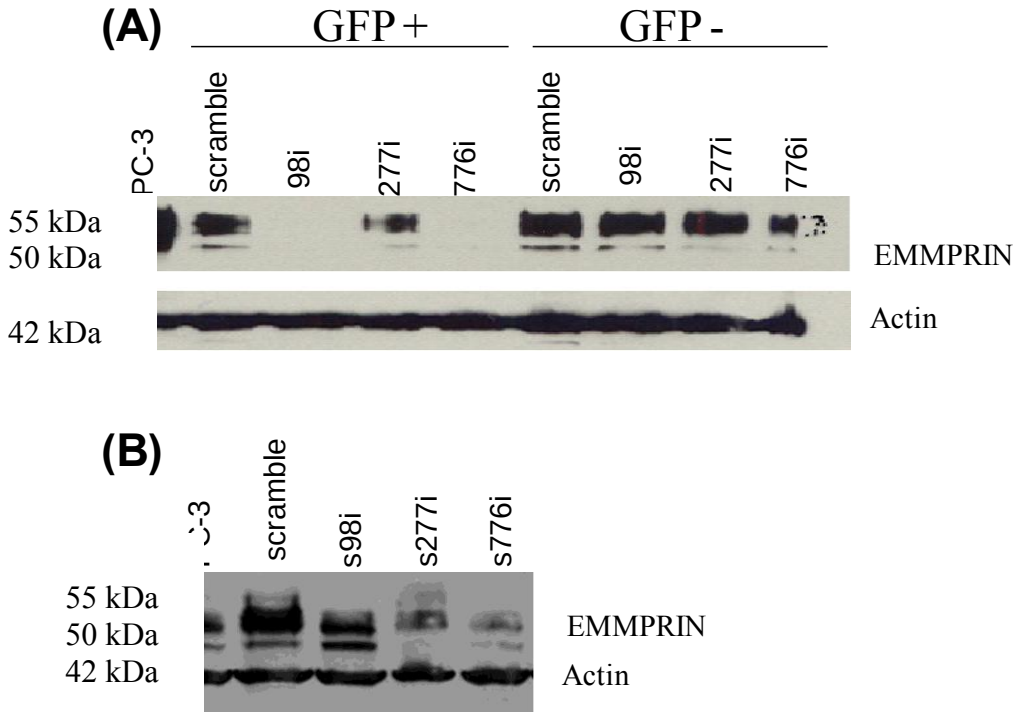
(A)
GFP +
GFP -
PC-3
scramble
98i
277i
776i
scramble
98i
277i
776i
55 kDa
50 kDa
42 kDa
EMMPRIN
Actin
(B)
scramble
s98i
s277i
s776i
55 kDa
50 kDa
42 kDa
EMMPRIN
Actin

Figure 3

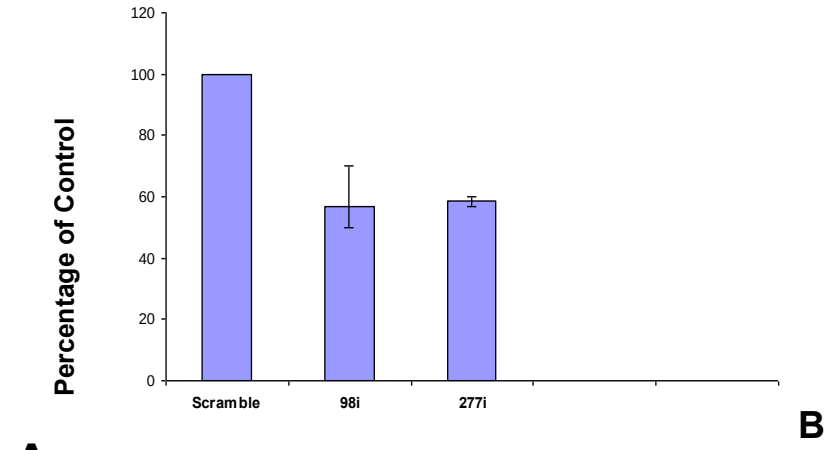

B

A

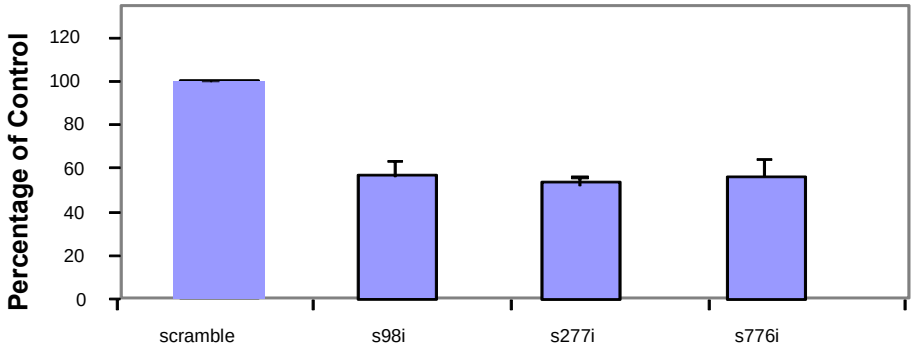

C

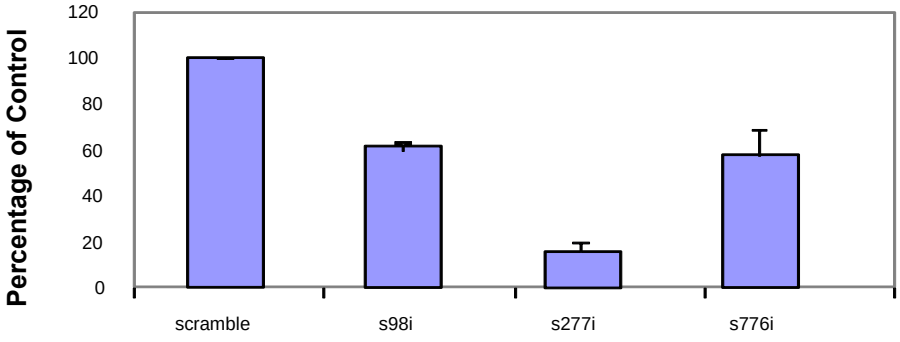

D

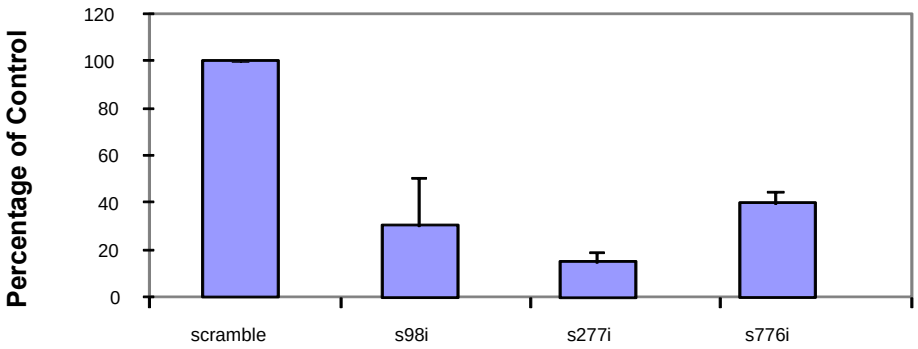

Figure 4

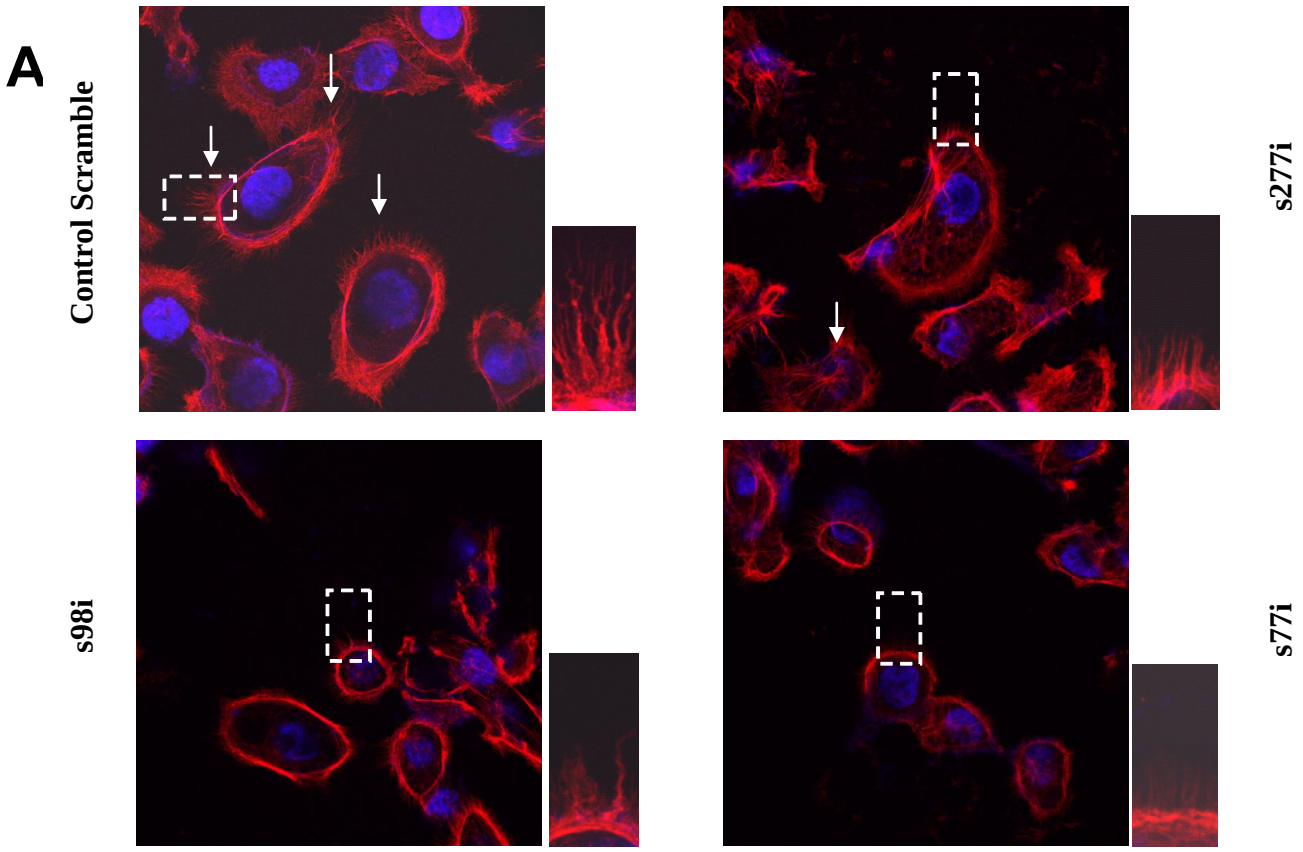
A
Control Scramble
s277i
s98i
s77i

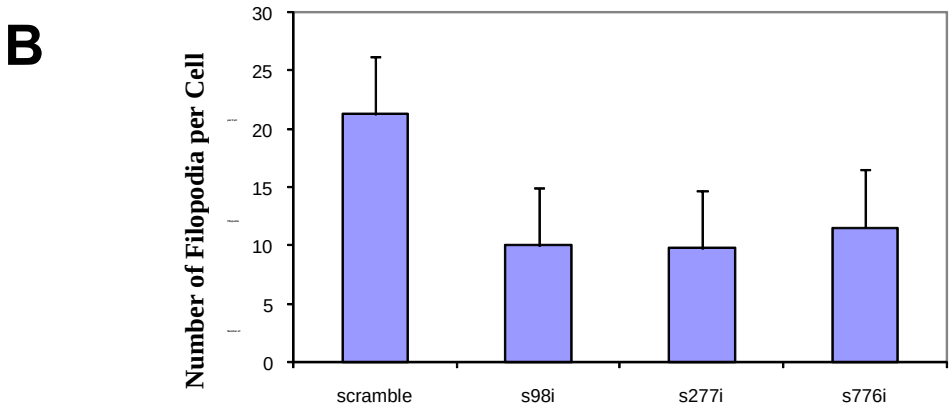
B
Number of Filopodia per Cell
30
25
20
15
10
5
0
scramble
s98i
s277i
s776i

Figure 5

A

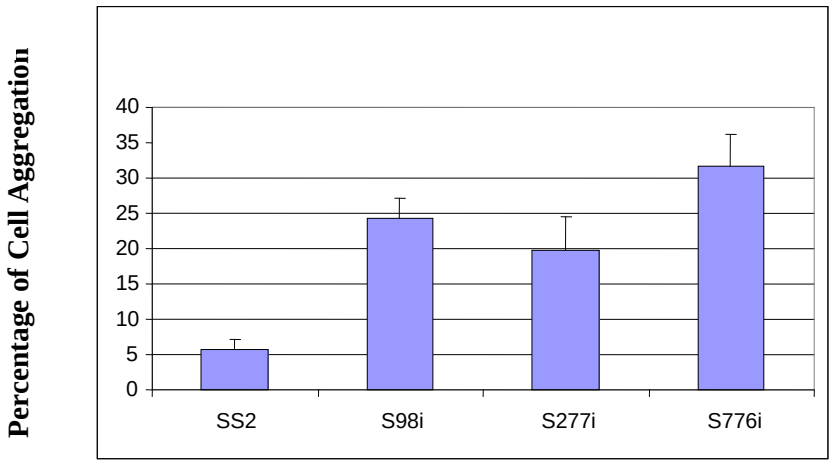
Percentage of Cell Aggregation
40
35
30
25
20
15
10
5
0
SS2
S98i
S277i
S776i

B

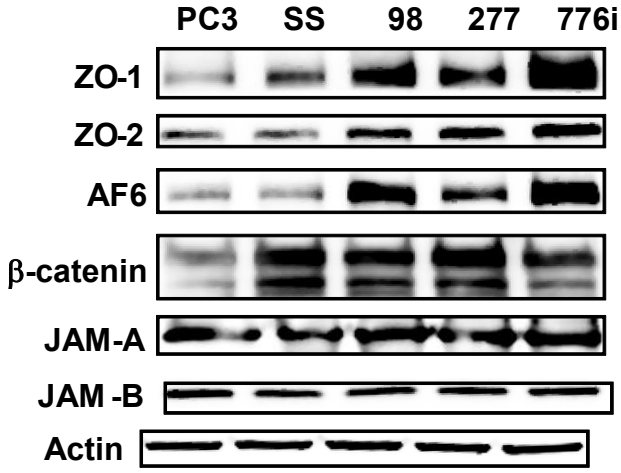
PC3
SS
98
277
776i
ZO-1
ZO-2
AF6
β-catenin
JAM-A
JAM -B
Actin

C

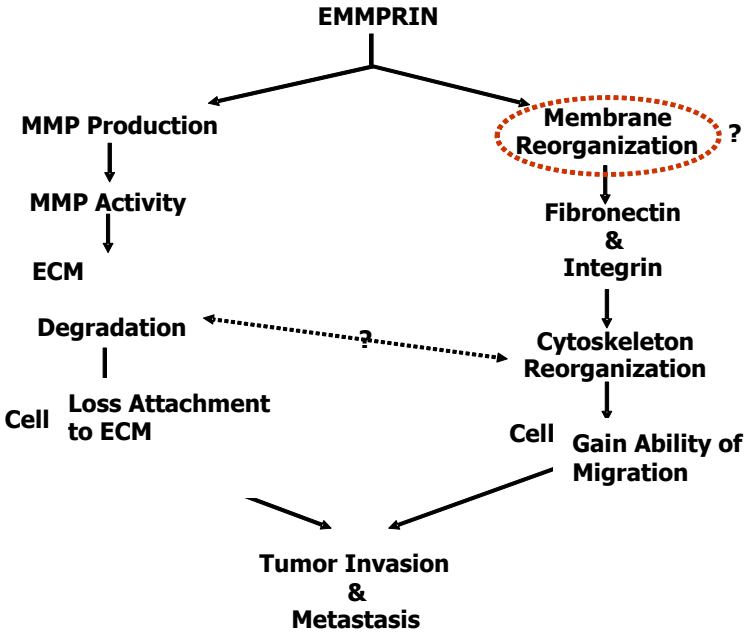
EMMPRIN
MMP Production
MMP Activity
ECM
Degradation
Cell
Loss Attachment
to ECM
Membrane
Reorganization
?
Fibronectin
&
Integrin
?
Cytoskeleton
Reorganization
Cell
Gain Ability of
Migration
Tumor Invasion
&
Metastasis

Supplementary Data

Figure S1. EMMPRIN silencing has no effect on prostate cancer cell proliferation, cell cycle progression and apoptosis. Panel A, Cell proliferation was assessed by the MTT assay as described in “Materials and Methods”**;** Panel B, cell cycle progression and Panel C, apoptosis in PC-3 EMMPRIN shRNA transfectants or scramble control cells were measured using the BrdU/PI double staining and TUNEL assays, respectively. The results shown represent the average values ± SEM, from three independent experiments.

Figure S1

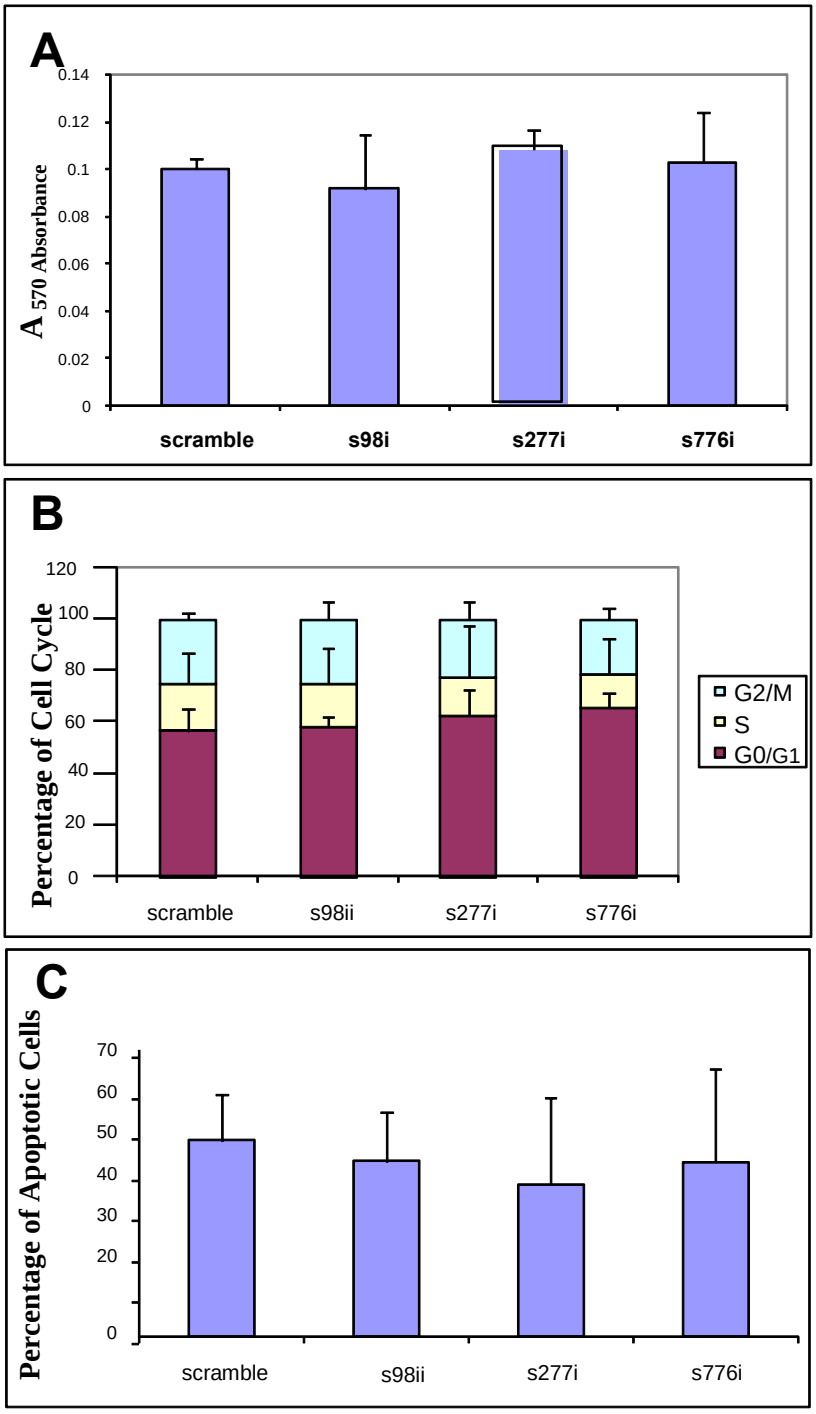
A
A 570 Absorbance
0.14
0.12
0.1
0.08
0.06
0.04
0.02
0
scramble
s98i
s277i
s776i
B
Percentage of Cell Cycle
120
100
80
60
40
20
0
scramble
s98ii
s277i
s776i
G2/M
S
G0/G1
C
Percentage of Apoptotic Cells
70
60
50
40
30
20
0
scramble
s98ii
s277i
s776i

Appendix 2

Cofilin, a Cytoskeleton Regulator of Transforming Growth Factor β (TGF-β), Mediates Prostate Cancer Cell Invasion and Metastasis

[1]Joanne Collazo, [2]Brian Zhu, [3]Craig Horbinski, [4]Hong Pu, [1]Roxana Loperena and Natasha Kyprianou[1, 2, 3, 4]

[1]Departments of Toxicology, [2]Department of Molecular and Cellular Biochemistry, [3]Department of Pathology , [4]Department of Urology, College of Medicine, University of Kentucky, Lexington, Kentucky.

Address correspondence to:
Dr. Natasha Kyprianou
Combs Cancer Building, Room 306,
University of Kentucky Medical Center,
800, Rose Street,
Lexington, KY 40536.

E-mail: nkypr2@uky.edu
Tel; 1859-323-9812

Running title: Role of TGF-β and Cofilin in Prostate Cancer Invasion and Metastasis

Key Words: prostate cancer, cofilin, cytoskeleton, filopodia.

Funding: NIH/NIDDK R01 #00491815 and DoD Award W81XWH-08-1-0431

Abbreviations : CFL, cofilin, TGF-β, Transforming Growth Factor Beta, EMT, Epithelial to Mesenchimal Transition, ECM, Extracellular Matrix, GFP, Green Fluorescent Protein, MTT, (3-(4,5-Dimethylthiazol-2-yl)-2,5-diphenyltetrazolium bromide, a yellow tetrazole), PMSF , phenylmethanesulfonylfluoride or phenylmethylsulfonyl fluoride, PBS, Phosphate Buffered Saline, SDS – PAGE, sodium dodecyl sulfate polyacrylamide gel electrophoresis**,** LIMK**,** Lim domain kinase.

Abstract

The actin depolymerizing factor (ADF) cofilin, a small (19kDa) actin binding protein was previously identified to be an intracellular effector of transforming growth factor beta (TGF-β) in prostate cancer cells (Zhu et al. 2006).This study investigated the consequences of a mutation in cofilin phoshorylation site Serine 3 residue; (S3ACFL) in human prostate cancer cell migration, and invasion, using the TGF-β sensitive, androgen-independent PC-3 cells as model. We comparatively evaluated cell migration and invasion potential in the wild type PC-3 cells, as well as the mutant S3A CFL PC-3 cells harboring the cofilin mutation, in the presence and absence of TGF-β. Our results demonstrated a significant increase in the migration ability for S3ACFL prostate cancer cells compared to the wild type controls. Furthermore there was enhanced adhesion to fibronectin in S3ACFL PC-3 cells, potentially driven by the significantly higher number of filopodia structures in cells harboring the cofilin mutation. TGF-β treatment (5ng/ml) led to a decrease in cell migration, adhesion and filopodia protrusions in the cofilin S3A cells. The mutation in cofilin phosphorylation site had no significant effect on the invasion potential of S3ACFL cells compared to wild type PC-3 cells. Human prostate cancer specimens from primary prostate tumors and lymph node metastatic lesions were analyzed by immunohistochemical analysis for the expression of cofilin, p-cofilin, palladin and e-cadherin. Cofilin immunoreactivity correlates with higher tumor grades and moreover there was a significant upregulation of cofilin in metastatic lesions compared to primary tumors. *In vivo* characterization of the metastatic potential of WTCFL and S3ACFL PC-3 cells revealed an increased number of lung metastatic

lesions for the mutants S3ACFL compared to wild type PC-3. These results suggest that a) cofilin promotes cytoskeletal reorganization of prostate cancer, thus facilitating metastastatic spread, b) TGF -β regulates activation/repression of cofilin's action and cell motility via "editing" actin cytoskeleton signalsand c) cofilin may have potential predictive value in prostate tumor progression to metastasis.

Introduction

According to the American Cancer Society (ACS), more than two million men in the United States had prostate cancer in 2012 with an estimated 241,740 new cases and 28,170 deaths due to the disease. 1 in 6 men will be diagnosed with prostate cancer during their lifetime; unfortunately 1 in 36 will not survive the disease. Death from prostate cancer results when cancer cells become metastatic and invade lymph and blood vessels and migrate to the lymph nodes and bone (Clarke et al. 2008). The only proven treatment conferring improved survival to patients with localized prostate cancer is androgen ablation therapy which involves either surgical or chemical castration. The apoptotic response to androgen ablation therapy in prostate cancer is the underlying mechanism for the therapeutic benefit due to tumor regression; what challenges this approach is the ability of prostate cancer cells to become resistant to androgen ablation, escape apoptosis and metastasize (Garison et al. 2004; McKenzie and Kyprianou 2006.) Taxane chemotherapy has been used for androgen independent prostate cancer. Increased overall survival has been demonstrated in studies utilizing the cytotoxic antimicrotuble drugs docetaxel, doxorubicin and paclitaxel. The higher overall survival has been obtained from docetaxel treatment; however, most of the patients show a limited duration of response to taxanes and therapeutic options are still limited after taxanes failure (Aragon-Chin et al. 2009).

The ability of cells to migrate is dependent on rapid polymerization and depolymerization of actin filaments (Yilmaz et al. 2010). The cellular cytoskeleton consists of a dynamic net of actin filaments which polymerization and

depolymerization allows the cell to move toward extracellular stimuli like growth factors and chemokines (Yilmaz et al. 2010). The ADF/cofilin protein is as small (19 kDa) actin binding protein that comprises the major regulator of the actin dynamics via the binding and severing of the filamentous form of actin. Binding of cofilin causes a reduction in the rotation of the actin filament resulting in a break and allowing a free barbed end for the addition of new actin monomers and generation of new actin filaments and filament branches (Van Troys et al. 2008, Ono S. et al. 2007, Hotulainen et al. 2005). Phosphorylation of cofilin on Ser3 by LIMK-2 inhibits its binding to G actin (monomeric actin) and F-actin (filamentous actin) and severing of the actin filament. The Rho-associated, coiled-coil containing protein kinase 1 (ROCK1), is responsible for the phosphorylation and activation of LIMK-2. Alterations in cofilin and its signaling effectors have been reported in invasive tumors from ovarian and breast cancer (Sadako et al. 2010).

Elevated transforming growth factor-β (TGF-β) is functionally linked to tumor progression via its role in increasing angiogenesis and decreasing immune responses (Teicher. et al. 2007). TGF-β signaling is propagated through two types of transembrane receptors (TβRI and TβRII) followed by downstream targeting through regulation of the SMAD family of protein effectors (Korpal et al. 2010). Previous work from this laboratory identified cofilin, as an intracellular effector of TGF-β (independent of Smads) in prostate cancer cells (Zhu et al. 2006). The present study investigated the functional consequences of a mutation in cofilin phoshorylation site (Serine 3 residue; S3ACFL) in human androgen-independent prostate cancer cells. Our

findings support a role for cofilin in regulating invasion and migration potential during prostate tumor progression.

Materials and Methods

Cell Culture and Treatment

The human prostate cancer cell line PC-3, was obtained from the American Type Culture Collection. The S3A cofilin mutant human prostate cancer cell line was generated by site directed mutagenesis in PC-3 cells. Briefly, a point mutation targeting Ser 3 phosphorylation site was induced by PCR. To mimic a dephosphorylated (constitutively active) form of cofilin (S3ACFL mutants), a substitution of a Serine on position 3 to Alanine was generated. Wild type and S3ACFL mutant forms of cofilin were introduced to PC-3 cells via stable transfection using Lipofectamine 2000 reagent (Invitrogen) according to the manufacturer's protocol. An S3DCFL PC3 cell line which mimics the constitutive phosphorylated (inactive) form of cofilin was generated via transient transfection as a control. Vectors for the expression of the S3D cofilin were generous gifts from Dr. Krupenko, Medical University of South Carolina, USA. Cells ($5x10^5$) were transfected with pXJN-HA/cofilin vector DNA (5.0 μg) using Effectene Transfection Reagent (QIAGEN 301425, Hilden, Germany).

Expression of mutant protein was detected by Western blot assays with cofilin-specific antibody, (Sigma Aldrich (3311), St. Louis, MO), (due to a HA-tag the mutant cofilin appears as a band migrating slower than 19kDa wild-type endogenous cofilin). siRNA technology was used to reduce cofilin expresion in PC-3 cells. The siRNA sequence targeting cofilin is designed from codons 64-84, relative to the start codon

(Dharmacon Research, Lafayette, CO). As control we used a siRNA containing a two single-nucleotide mutation of the cofilin sequence (C71G and A73U). Immunoflurorescence microscopy was subsequently applied to determine whether expression was reduced. Cells were maintained in RPMI 1640 (Gibco ^{TM}, Grand Island NY), supplemented with 10% fetal bovine serum, 100 units of penicillin, and100 mg/mL streptomycin. Subconfluent cultures were treated with TGF-β (R&D Systems, Minneapolis, MN) (5ng/ml, as described for individual experiments).

Cell Viability

To determine cell viability in response to two different mutations in cofilin protein (S3A, TR25A), or cofilin silencing; the colorimetric MTT metabolic activity assay was used. WT CFL, shCFL and mutant S3ACFL PC-3cells (1×10^4 cells/well) were cultured in a 96-well plate at 37 °C. After 24 hrs supernatants were removed and individual wells were washed with Phosphate Buffered Saline (PBS). Subsequently 20 µl of MTT solution (5 mg/ ml in PBS) was added to each well followed by 100 µl of medium(4 hrs).The resultant formazan crystals were dissolved in dimethyl sulfoxide (100 µl) and the absorbance intensity measured by a microplate reader (Bio-RAD 680, USA) at 490 nm with a reference wavelength of 620 nm. All experiments were performed in triplicates, and the relative cell viability (%) was expressed as a percentage relative to the control WT CFL PC-3cells.

Western Blot Analysis

Cell pellets from each prostate cancer cell line and metastatic lung tissue homogenates were lysed in RIPA buffer (50mM Tris-HCl, pH7.4, 1%NP40, 0.25% Na-deoxycholate, 150 mM NaCl, 1mM EDTA, 1mM PMSF, Sigma P8340 protease inhibitor cocktail 1:100). Lysates were subjected to centrifugation at 2,400 RPM (15 min), resolved by SDS-PAGE, and transferred to Immun-Blot PVDF membranes (0.2μm) for protein blotting (Bio - Rad 162- 0177). Upon incubation with primary antibody, bands were detected using a chemiluminescent approach with a GE ECL plus Western Blot Detection System (GE, Amersham, UK). Total cofilin and p-cofilin proteins were detected using the following antibodies: (C8736) Anti - cofilin from Sigma Aldrich, (3311)(St. Louis, MO), Phospho–cofilin (Ser 3) from Cell Signaling Technology (Danvers, MA). LIMK-2 was detected using the (3844) LIMK-2 antibody, (Cell Signaling). GFP expression was detected using sc-GFP antibody (sc-8334) (Santa Cruz Biotechnology, Santa Cruz, CA).

Migration Assay

WTCFL, S3ACFL and S3DCFL PC-3 cells were seeded in 6-well plates and 60-70% density cell monolayers were wounded and exposed to TGF-β (5ng/ml; 24 hrs). The number of migrating cells was evaluated and counted in three different fields under microscopic examination.

Invasion Assay

The invasion potential of prostate cancer cells was evaluated using a Biocat Matrigel Transwell Chamber (Beckon Dickinson, Franklin Lakes, NJ). Cells were seeded into the upper chamber of a transwell insert pre-coated with EMC in serum-free medium at a density of 50,000 cells/well. Culture medium containing fibronectin (5µg/ml) was placed in the lower chamber as an adhesive substrate and cells were incubated for 24 hrs in a (5% CO_2) incubator. Non-invading cells were removed from the upper chamber by scraping with a swab and cells that have invaded were stained with Diff-Quick Solution (IMEB Inc., San Marcos, CA) and counted in five random fields.

Adhesion Assay

Wild type and S3ACFL mutants PC-3 cells were treated with TGF-β (5ng/ml, 24 hrs) at 37ºC. Cells (40,000 cells/well) were seeded in 6-well plates pre-coated with fibronectin (0-8 µg/ml). After 30 min incubation (at 37ºC) non adherent cells were removed and adherent cells were fixed. The number of cells attached was evaluated in three different fields under microscopic examination.

Immunofluorescence Staining

Cells (7 x 10^4cells/well) seeded in 6-well plates with a glass coverslip were exposed to TGF-β (5ng/ml, 24 hrs) at 37ºC. Cells were subsequently fixed with methanol-free formaldehyde (3.7% v/v) and permeabilized with Triton X-100 (0.1% v/v). After blocking for1hr (PBS/Normal Goat Serum/0.3% Triton X-100) fluorescent staining of filamentous actin was performed using Rhodamine Phalloidin staining of F-actin

according to the manufacturer's instructions (Invitrogen, Grand Island, NY). Cofilin expression was detected by incubating cells with (C8736) Rabbit Anti - cofilin antibody (Sigma) following incubation with Alexa Fluor 488 (Invitrogen) (24hrs). Images were captured and processed using an epifluorescence Nikon Eclipse E600 microscope. The images were capture using a Spot charge coupled device camera system (Nikon, Melville, NY).

Immunohistochemical analysis

Formalin- fixed paraffin- embedded specimens of human local and metastatic prostate cancer (n=11), were obtained from the University of Kentucky Cancer Center Tissue Biobank with Institutional Review Board Approval. Sections (4µm) were affixed to glass slides, deparafinized and rehydrated. Total cofilin and p-cofilin expression was detected using the following antibodies: (C8736) Anti - cofilin from Sigma Aldrich, (3311) Phospho – cofilin (Ser 3) from Cell Signaling Technology. Palladin expression was detected using (10853-1-AP) PALLD palladin antibody (Proteintech Group Inc., Chicago, IL). E- Cadherin expression was detected using (24E10) E-Cadherin rabbit antibody (Cell signaling, Danvers, MA). Sections were incubated with the corresponding primary antibodies (1:50 to 1:100) (24hrs); were subsequently exposed to Millipore (21537) (EMD Millipore Corporation, Billerica, MA,) IHC select immunoperoxidase secondary detection system (1hr) followed by incubation with Millipore Streptaviding HRP (1hr). Peroxidase activity was detected by applying Diaminobenzidine (DAB) and counterstained with hematoxylin. Slides were analyzed under a light microscope followed by pathological evaluation. For H-score assessment

three fields were selected at random at 40x magnification and the staining intensity in the malignant cell nuclei was scored as from 1 to 10 , corresponding to the presence of negative, weak, intermediate, and strong brown staining, respectively. The percentage of stained cells in each field (Q) and the number of cells stained at each intensity (I) were counted by two different observers. A score for each defined histological category (H) was determined as the product of the intensity and proportion (I+Q).

Experimental Metastasis Assay

The metastatic potential of WTCFL and S3ACFL mutant PC-3 cells was studied by tail vein injections. Male nude mice (6-wks old) (Harlan Laboratories Inc., Indianapolis, IN) were maintained in sterile plastic cages on in an air-conditioned, pathogen-free animal room at 22 - 28C and 50% humidity with 12:12 hr light/dark cycle. The animal experiments were performed under protocols approved by the Institutional Animal Care and Use Committee. GFP labeled WTCFL and S3ACFL mutant PC-3 cells ($1x10^6$) were injected into the tail vein of mice (n=6 for each cell line). At 4-weeks post inoculation, lungs were surgically excised and metastatic lesions to the lungs were examined under the microscope. Lung tissue was homogenized and lysed in RIPA buffer for western blot for the detection of GFP, cofilin and p-cofilin.

Statistical Analysis

All statistical analyses were performed with GraphPad Prism 5 for Windows (GraphPad Software, San Diego, CA). Data are presented as means $\pm$SEM. Quantitative bar graphs from prostate cancer cell migration, invasion and cell attachment are shown

in figures. Values shown are the mean of three independent experiments performed in triplicates. Significant difference was defined at *P value < 0.05 when compared to control. Statistical evaluation of the different groups was performed using the Student *t* test and Two Way Analysis of Variance for multiple comparisons.

Results

Cofilin Expression in Human Prostate Cancer Cell Lines

Via the substitution of a Serine on position 3 to Alanine it was possible to mimic a dephosphorylated form of cofilin (S3ACFL mutants). Profiling of protein levels for total cofilin, phosphorylated cofilin and LIMK-2 total expression was conducted in wild type PC-3 cells versus mutant PC-3 cells bearing the constitutive dephosphorylated (active) form of cofilin (S3ACFL) by Western blotting. As shown in Figure 1 (lanes 1 and 7), the mutation in cofilin phosphorylation site Ser 3, had no effect on cofilin total expression, but it impaired cofilin phosphorylation by LIMK-2. An increase in LIMK-2 was found in mutant S3ACFL PC-3 cells compared to wild type (Fig. 1). Since cofilin is an intracellular effector of TGF-β (Zhu et al. 2006), we investigated whether TGF-β modulates cofilin phosphorylation state in prostate cancer cells. Treatment with TGF-β (for 6 hrs) leads to an upregulation of ROCK1, LIMK-2, as well as phosphorylated cofilin in the wild type cells, while there was a significant reduction in LIMK-2 in mutant S3ACFL cells (Fig 1, Panels A and B).

Effect of TGF-β on Increased Migration in Mutant S3A Cofilin Prostate Cells

To determine the effect of a mutation in cofilin phosphorylation site on prostate cancer cell migration, we comparatively assessed the migration ability of wild type and

mutants S3A and S3D cofilin mimicking the constitutive active and inactive forms of cofilin respectively. The results in Figure 2 revealed a significant increase in migration ability for the mutant S3ACFL PC-3 cells, compared to wild type, (Panels A and C). Treatment with TGF-β (5ng/ml, 24 hrs) leads to a reversion to the wild type phenotype for the mutant S3ACFL, (Fig. 2, Panels B and C).

S3ACFL has no Significant Effect on Prostate Cancer Cell Invasion

The impact of S3ACFL on the invasion of prostate cancer cells was examined next. The data shown on Figure 4 indicate that there was no significant effect in the invasion potential of S3A cells compared to controls. TGF-β treatment (24hrs) led to an increased number of invading cells in both cofilin and mutant cells.

Effect of S3A Mutation on Cell Adhesion and Filopodia Formation

Cell adhesion is directly dependent on cofilin activity and cytoskeletal actin reorganization since depolimeryzation and polymerization of new actin filaments is required for the formation of filopodia (Arjonen et al. 2011). To investigate the effect of S3A mutation on cell adhesion and filopodia formation, we examine the adhesion ability of wild type and S3ACFL mutants PC-3 cells to fibronectin, a key component of the extracellular matrix. There was an increase in cell attachment for the mutant S3ACFL that correlates with increased filopodia protrusions, as assessed by fluorescence staining of F actin with rhodamine phalloidin, (Fig.4, Panel A and Figure 5, Panel A). High cofilin expression was detected at the cell membrane in areas were there was a prominent presence of filopodia structures (Figure 5, panel B). Exposure to

TGF-β reduced the adhesion ability of cell to fibronectin, (Figure 4, Panel C) while it resulted in a decreased number of filopodia structures for the mutant S3ACFL cell line (Figure 5, Panels C and D).

S3ACFL mutation enhances *in vivo* PC-3 cell metastasis

The experimental metastasis assay revealed an increased in the *in vivo* metastatic ability of mutant S3ACFL, compared to WTCFL prostate cancer cells based on the metastatic lesions to the lungs after the tail - vein injection (Figure 6).

Cofilin Overexpression Correlates with Human Prostate Cancer Progression

Immunohistochemical profiling of cofilin on human prostate cancer patients with localized and metastatic disease to the lymph nodes revealed higher cofilin expression for metastatic tissue compared to primary in all of the cases (n=11). Characteristic images reveal intense cofilin staining in tissue from lymph node metastasis (Fig. 6, Panel B). A weak cofilin expression was detected in highly differentiated prostate tumors compared to grades 3 and higher. As shown on Figure 6, (Panels A and B), there was strong cofilin immunoreactivity in poorly differentiated tissue where metastatic prostate tumor cells were able to disrupt the actual glands invading the stroma.

Discussion

This study pursued characterization of actin remodeling protein cofilin and its interaction with TGF-β, a major regulator of the tumor microenvironment. Our findings indentified a functional contribution of cofilin to the metastatic process in prostate

cancer. The results revealed significant differences in migration, invasion and adhesion potential between the wild type and mutant (constitutively active) S3ACFL PC-3 expressing a mutant cofilin phosphorylation site. S3ACFL conferred an increase in the migration potential compared to wild type PC-3 cells, suggesting that cofilin regulation is functionally linked to the acquisition of an enhanced migratory phenotype in prostate cancer cells. One may argue that the mutation does not significantly impact prostate cancer cell invasion since cofilin activity is directly responsible for the remodeling of actin filaments toward cytoskeletal reorganization, thus driving cell motility (but not invasion).

Cell migration relies on the coordinated remodeling of the actin cytoskeleton and leading edge protrusions of moving cells are formed by special actin structures known as lamellopodia and filopodia. (Arjoen et al. 2011). Experimental studies on mammary carcinoma cells reveal that stimulation by epidermal growth factor (EGF) activates cofilin, increasing the number of actin filament barbed ends. The elongation of barbed ends via the polymerization of G actin monomers generates new actin filaments and filament branching adjacent to the plasma membrane at the tip of the leading edge (Zebda et al. 2000). The study revealed an increased filopodia formation in the mutant S3ACFL, suggesting that alterations in cofilin phosphorylation site in prostate cancer cells may interfere with the functional of the protein. Cofilin disregulation leads to enhanced actin severing increased cytoskeletal remodeling and formation of new filopodia. Filopodia can provide not only enhanced cell motility, but also facilitate attachment to the ECM and to a distal site promoting colonization and formation of secondary tumors (Arjonen et al. 2011). Our findings support the notion

that a mutation in cofilin regulation site, besides enhancing cell movement, it can also increase cell adhesion to fibronectin, a key component of the ECM in mutant S3ACFL PC-3 cells.

Previous data from this laboratory established cofilin as a Smad independent effector of TGF- β (Zhu et al. 2006). Interestingly enough, in this study we found that pretreatment with TGF-β leads to a reversion to the wild type phenotype for the mutant S3ACFL. In response to TGF-β there was a decrease in cell migration and adhesion in the mutant cofilin S3A cells. As cofilin is unable to be phosphorylated by LIMK-2 in S3ACFL mutants, our findings suggest an alternative pathway via which TGF-β is modulating cofilin activity and exerting its role as a tumor suppressor in these cells. One may argue that TGF-β transduction is no longer exclusively targeted to the modulation of cofilin severing activity at the cell membrane in these cells. Considering this scenario in response to TGF-β, mutant cofilin translocates to the nucleus, and can mediate actin remodeling facilitating the intranuclear trafficking of proteins and binding of transcription factors complexes leading to repression of TGF-β responsive genes. TGF-β may mediate prostate cancer progression via non-Smad (noncanonical) pathway, by inhibiting cofilin activity provided by a mutation on cofilin Ser 3 phosphorylation site. This supports a role of cofilin as an effector for Smad independent TGF-β signaling in prostate cancer progression towards metastasis, possibly navigating the functional swinging of TGF-β from tumor suppressor to a metastasis promoter in late stages of tumorigenesis.

Dynamic interactions between cancer cells and the stroma microenvironment (inflammatory cells, vessels, fibroblasts and components of the ECM) impact tumor

invasion (Desmoulière et al 2004, De Wever and Marel 2003). One could easily argue that impairing cofilin's activity (due to spontaneous mutations on phosphorylation site), is an early event leading to an enhanced migratory potential of prostate cancer cells towards metastasis. This is the first evidence to suggest that induced cofilin severing activity facilitates prostate cancer cells adhesion to the ECM and enhances tumor cell migration. Interestingly we found an increased in cell invasion after treatment with TGF- β in both cell lines, implicating TGF-β as one of the active components in the surrounding stroma influencing tumor progression and invasion. In early stages of tumorigenesis when cancer cells are confined as a primary tumor, TGF-ß as a protagonist of the tumor microenvironment, serves as a defense mechanism to block cancer cell spreading to distal parts of the body. TGF-ß exerts its tumor suppressor role by activating the RhoA/ROCK1 signaling pathway, leading to the phosphorylation and activation of LIMK-2; impairing cofilin severing activity, cytoskeletal reorganization and formation of filopodia and lamellopidia, ultimately decreasing cell motility.

Dynamic changes in cofilin expression have been reported in several human malignancies like colon and ovarian cancer (Wang et al. 2007, Sadako et al. 2010, Agnieska Popow et. al 2012). Immunohistochemical profiling of human metastatic prostate cancer tissue revealed high cofilin expression in lymph node tissue suggesting a role of cofilin in facilitating the spreading of prostate cancer cells via the lymph system. Consistent with our results, increased cofilin levels were detected in metastatic prostate cancer specimens compared to their primary tumors counterparts from the same patient cohort. The loss of the epithelial marker E-cadherin, a cell adhesion

protein that plays an important role in normal growth and development is associated with a more invasive phenotype in prostate cancer cells and has been found to be reduced or absent in high grade prostate cancer (Umbas et al. 1992).In accordance a relatively low E-cadherin immunoreactivity was detected in the majority of primary prostate cancer specimens compared to metastasis confirming the progression of the disease to a more aggressive stage. Interestingly we found E- cadherin expression to be recovered in the metastatic stage of the disease. Our data resonate with recent studies by Nishimura et al, that reported a correlation between cofilin expression with epithelial ovarian cancer progression, revealing longer progression free survival in cofilin low-expression cases than in high-expression cases (Nishimura et al. 2011).

In summary the strong correlation between cofilin overexpression with the *in vitro* metastatic and *in vivo* invasive behavior of prostate cancer cells provides a new insight into the role of this protein in prostate cancer progression to metastasis.

Figure Legends

Figure1. Effect of S3A Mutation on Cofilin Expression and Phosphorylation in rostate Cancer Cells

Expression of cofilin, p-cofilin and LIMK-2 proteins. Panel A, Western Blot indicating increase in LIMK-2protein levels in mutant cells. Treatment with TGF-β (5ng/ml) increased total LIMK-2 and p- cofilin expression in the wild type and decreased the expression of LIMK-2 for the mutant cell line. Panel B, Western Blots indicating elevated RhoA and ROCK1 kinase protein level in mutant PC-3, (S3D cofilin double band due to a HA-TAG on mutant S3DCFL PC-3). Panel C, TGF-β (9hrs) increased RhoA and ROCK1expression in wild type PC-3 cells and decreased the expression of both proteins in the mutant cells. GAPDH was used as a loading control.

Figure2. Function of Cofilin in Prostate Cancer Cell Viability

Cell viability of PC-3 cells was not significantly affected by the introduction of two different mutations in cofilin protein (S3A, TR25A), or cofilin silencing by shRNA (ShCFL1).

Figure 3. Cofilin S3A Mutation Enhances Prostate Cancer Cell migration.

Wt CFL, S3A CFL and S3D CFL mutant prostate cancer cells were seeded in 6 well plates and a wound was induced. Panel A, increased cell migration on mutant S3ACFL PC-3. The number of cells migrating to the wound was counted in three different fields (after 24 hrs).Values shown are the mean of three independent experiments performed in triplicates (*p‹ 0.05 compared to WT CFL control). Panels B,C, TGF-β decreased

cell migration in the mutant S3ACFL cells while S3DCFL mutation decreases PC-3 cell migration. Panel D, the mutation in cofilin phoshorylation site did not affect the invasion potential of PC-3 cells.TGF-β (5ng/ml; 24hr) has no significant effect in the invasion potential for WTCFL and mutant S3ACFL PC-3 cells. Values shown are the mean of three independent experiments performed in triplicates. Statistical significance was set at a value of *p‹0.05.

Figure 5. Effect of S3A Mutation on Cell Adhesion to Fibronectin

Panel A reveals increased number of cells attached to a fibronectin coated plate for the mutant S3ACFL's cells. Values shown are the mean of three independent experiments performed in triplicates (*p‹ 0.05 compared to WT CFL control). Panel B reveals that TGF-β decreased cofilin mutant cell adhesion. Values shown are the mean (+/-SEM) of three independent experiments performed in triplicates. Statistical significance was set at a value of *p‹0.05.

Figure 6. S3A Cofilin Mutation Enhances Filopdia Formation

Panel A indicates representative images of confocal microscopy showing increased number of filopodia structures in mutant cofilin PC-3. Panel B, cofilin/rhodamine phalloidin coimmunostaining showing cofilin (green) colocalization with filopodia structures (red). Panels C, D, TGF-β treatment (5ng/ml; 24 hrs) decreased filopodia protrusions in mutant cells (arrows showing actual filopodia). (Inserts represent a zoom-in of region in boxed areas).

Figure7. Immunostaining Profiling of Cofilin in Human Prostate Cancer Specimens

Panel A indicates representative images of immunohistochemical staining for cofilin, p-cofilin, e- cadherin and palladin on primary and metastatic prostate cancer. Panel B, strong cofilin immunoreactivity in metastatic tissue which correlates with higher grade of disease. Panel C, representative images of lymph node metastatic tissue showing intense cofilin staining at the lymph node area. Panel D, quantitative analysis (H scoring) of immunostaining for specific proteins as indicated. The immunostaining results were scored incorporating both the intensity of staining (I) and the number of positively stained cells (Q). A score for each defined histological category (H) was determined as the product of the intensity and proportion (I+Q).

Figure 8. Experimental Metastasis Assay

Male nude mice (n=12) were injected with Wild type GFP labeled or mutant GFP labeled S3ACFL PC-3 cells via tail vein. Higher number of lung metastasis lesions (4 weeks after injection) were found in mice injected with S3ACFL PC-3 cells compared to control. The data shows the actual number of metastatic lesions to the lung per mouse for both (WTCFL and S3ACFL PC-3) injected groups. Statistical significance was set at a value of $p^{*}<0.05$.

Figure 1

A.

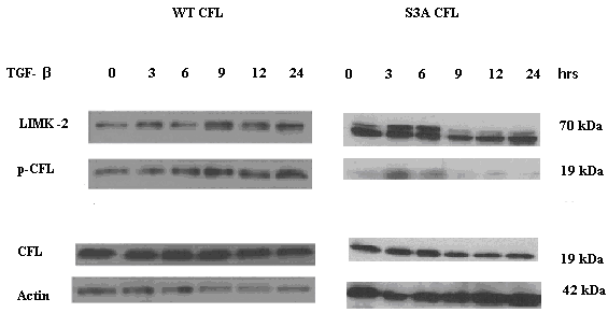
WT CFL
S3A CFL
TGF- β
0 3 6 9 12 24
0 3 6 9 12 24 hrs
LIMK -2
70 kDa
p-CFL
19 kDa
CFL
19 kDa
Actin
42 kDa

B.

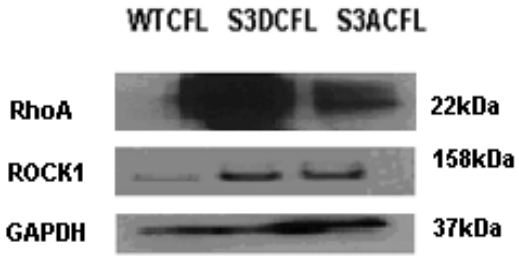
WTCFL S3DCFL S3ACFL
RhoA
22kDa
ROCK1
158kDa
GAPDH
37kDa

C.

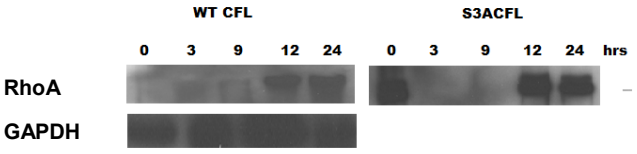
WT CFL
S3ACFL
0 3 9 12 24
0 3 9 12 24 hrs
RhoA
GAPDH

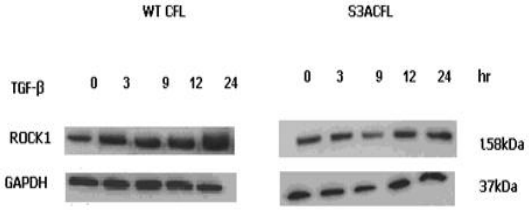
WT CFL
S3ACFL
TGF-β
0 3 9 12 24
0 3 9 12 24 hr
ROCK1
158kDa
GAPDH
37kDa

Figure 2.

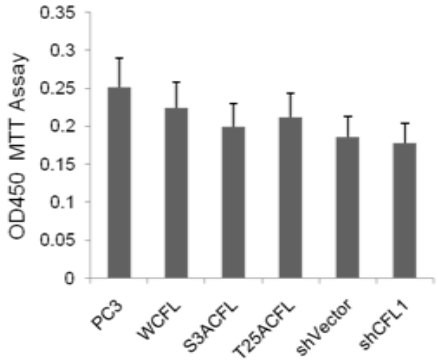

Figure 3.

A.

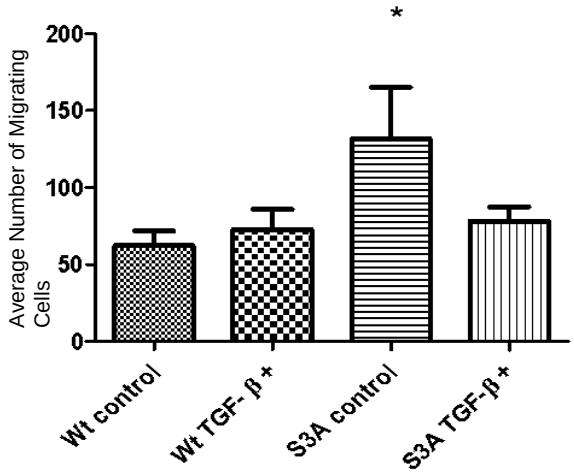

B

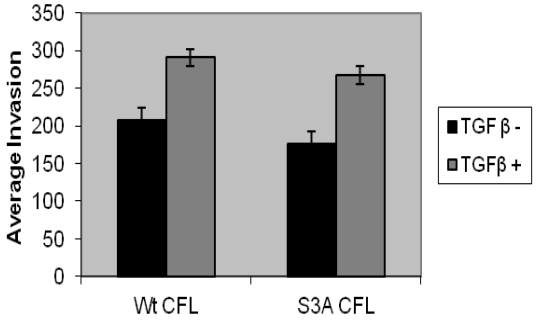

Figure 4

A.

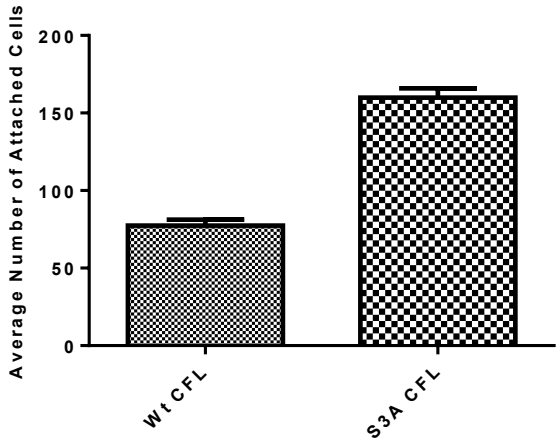
Average Number of Attached Cells
200
150
100
50
0
Wt CFL
S3A CFL

B.

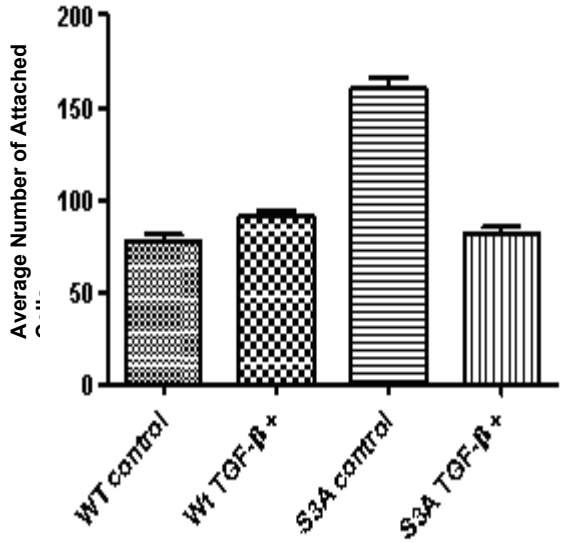
200
150
100
50
0
WT control
Wt TGF-β+
S3A control
S3A TGF-β+

Figure 5

A.

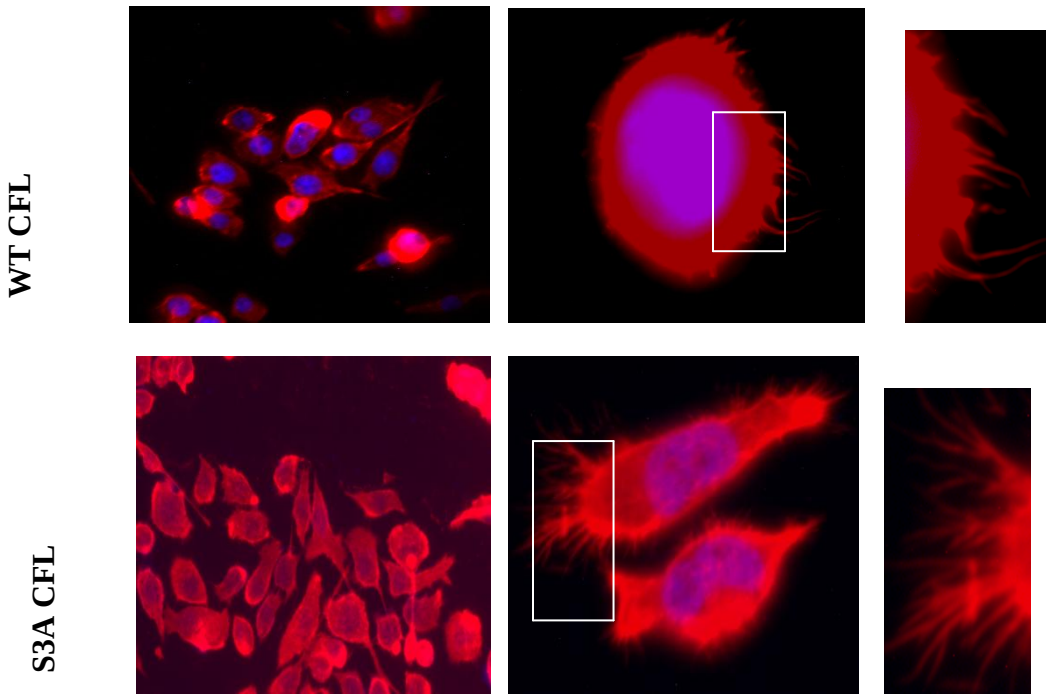

B.

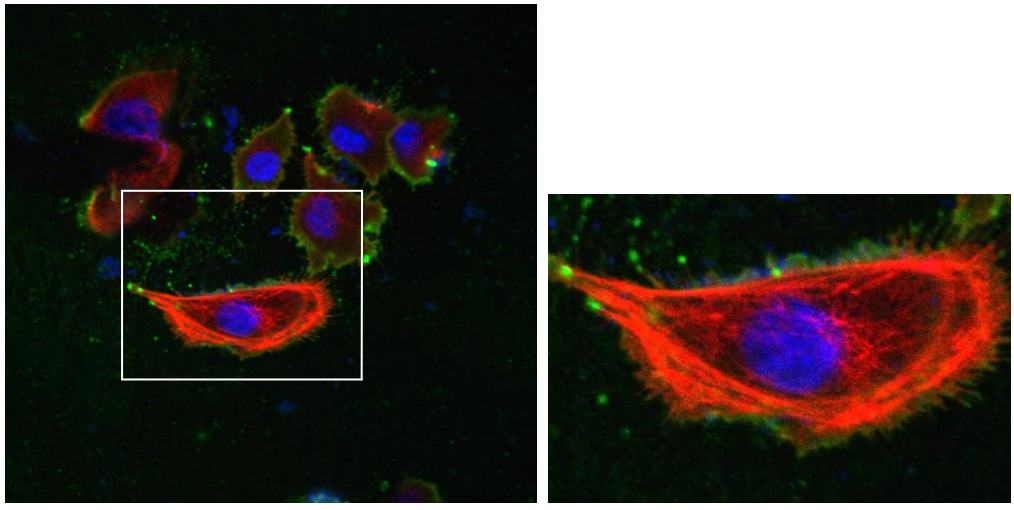

C.

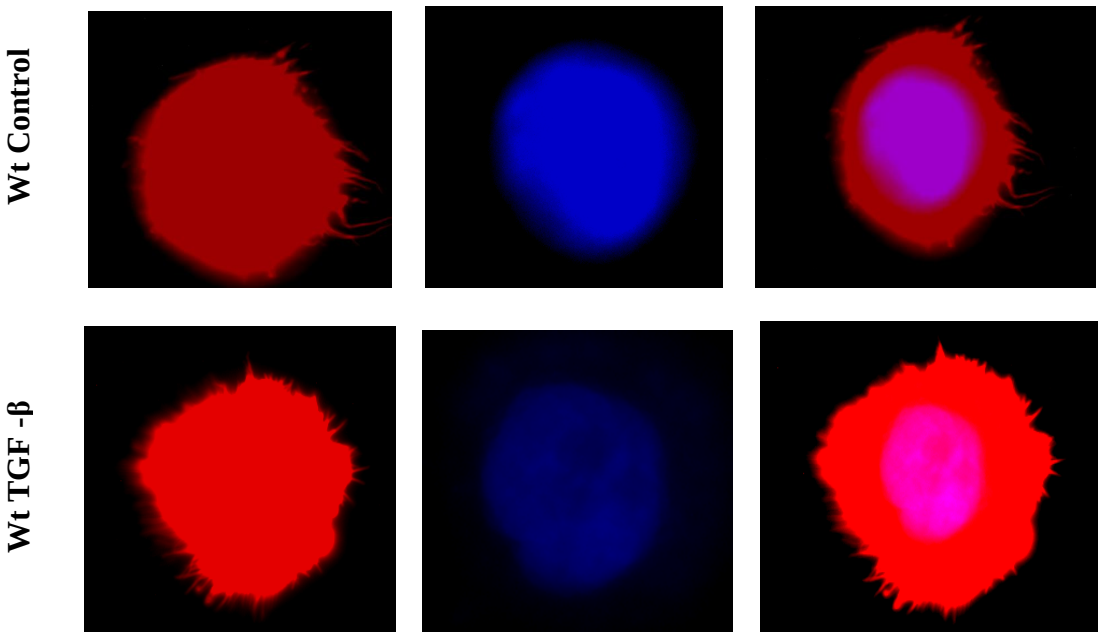

D.

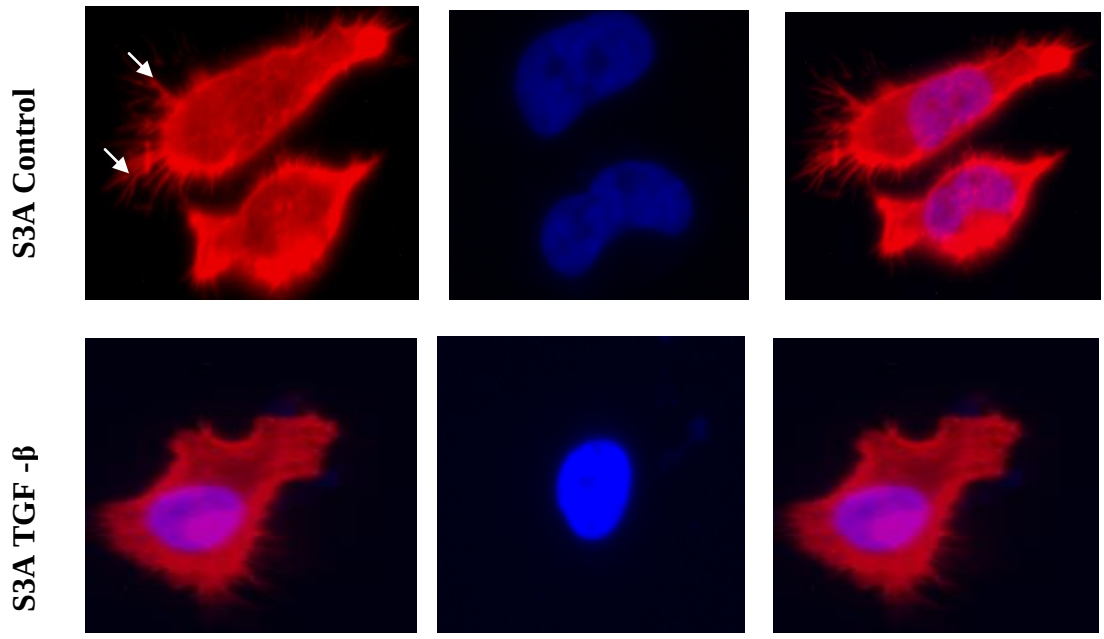

Figure 6

A.

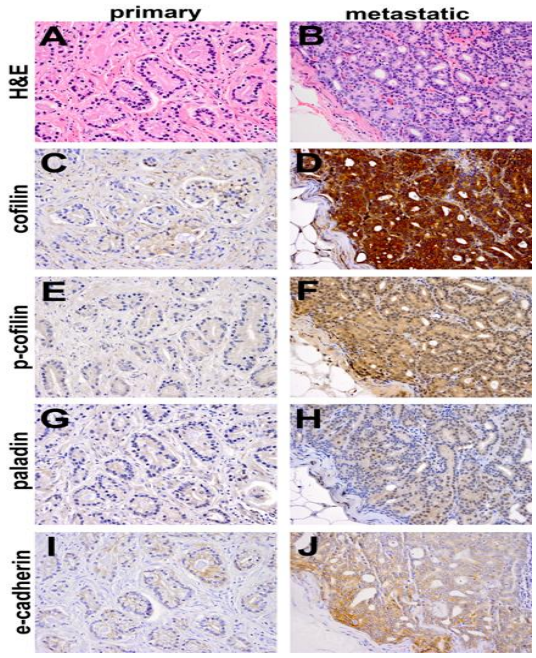

D.

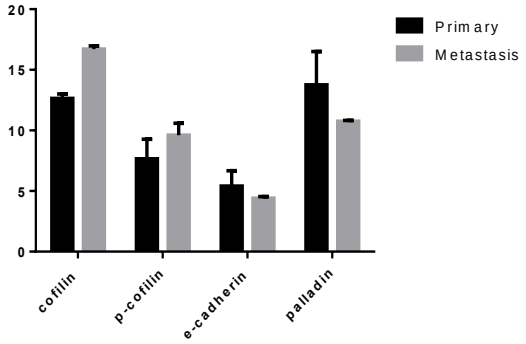

B.

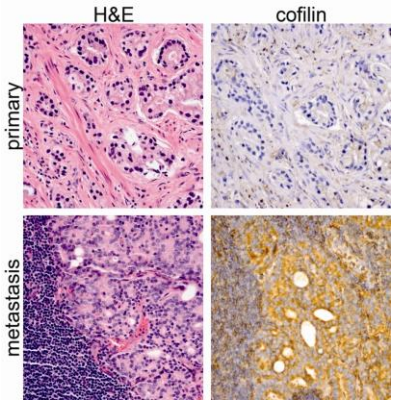

C.

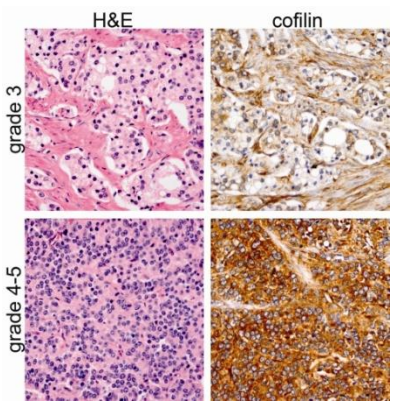

Figure 7.

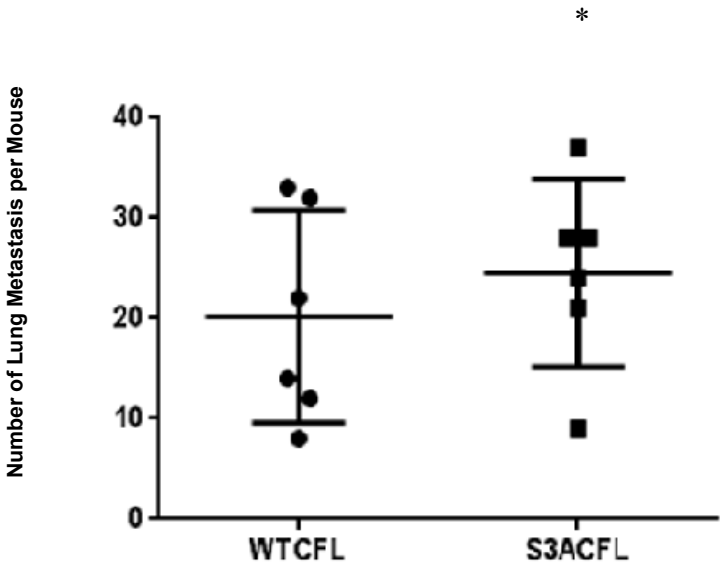
*
Number of Lung Metastasis per Mouse
40
30
20
10
0
WTCFL
S3ACFL

References

1. Aragon-Ching JB, Dahut WL. 2009. Chemotherapy in Androgen-Independent Prostate Cancer (AIPC): What's next after taxane progression? Cancer Ther.; 5A:151-160.

2. Arjonen A, Kaukonen R, Ivaska J. 2011. Filopodia and adhesion in cancer cell motility. Cell Adh Migr; 5(5):421-30.

3. Beibei Zhu, Kei Fukada, Haining Zhu, and Natasha Kyprianou. 2006. Prohibitin and cofilin are intracellular effectors of transforming growth factor beta signaling in human prostate cancer cells. Cancer Res.; 66(17):8640-7.

4. Bello-Deocampo, D. & Tindall. 2003. D.J. TGF-b/Smad signaling in prostate cancer. Curr. Drug Targets; 4, 197–207.

5. Chen J, Godt D, Gunsalus K, Kiss I, Goldberg M, Laski FA. 2001. Cofilin/ADF is required for cell motility during Drosophila ovary development and oogenesis. Nat Cell Biol.; 3(2):204-9.

6. Condeelis J, Singer RH, Segall J .2005.The great escape: when cancer cells hijack the genes for chemotaxis and motility. Annu Rev Cell Dev Biol.;21:695-718

7. Davila M, Frost AR, Grizzle WE, Chakrabarti R. 2003. LIM kinase 1 is essential for the invasive growth of prostate epithelial cells: implications in prostate cancer. J Biol Chem.; 278(38):36868-75.

8. Desmoulière A, Guyot C, Gabbiani G. 2004. The stroma reaction myofibroblast: a key player in the control of tumor cell behavior Int J Dev Biol.; 48(5-6):509-17.

9. Ellenrieder V. 2008. TGFbeta regulated gene expression by Smads and Sp1/KLF-like transcription factors in cancer. Anticancer Res.; 28(3A):1531-9.

10. Garrison JB, Kyprianou N. 2004. Novel targeting of apoptosis pathways for prostate cancer therapy. Curr Cancer Drug Targets; 4(1):85-95

11. Gupta GP and Massagué J .2006. Cancer metastasis: building a framework. Cell 127(4):679-95.

12. Goustin AS, Leof EB, Shipley GD, Moses HL. 1986. Growth factors and cancer. Cancer Res ; 46(3):1015-29.

13. Ghosh M, Song X, Mouneimne G, Sidani M, Lawrence DS, Condeelis JS. 2004. Cofilin promotes actin polymerization and defines the direction of cell motility. Science; 304(5671):743-6.

14. Hall A. 1994. Small GTP-binding proteins and the regulation of the actin cytoskeleton. Annu Rev Cell Biol. ; 10:31-54.

15. Hotulainen P, Paunola E, Vartiainen MK, Lappalainen P. 2005. Actin-depolymerizing factor and cofilin-1 play overlapping roles in promoting rapid F-actin depolymerization in mammalian nonmuscle cells. Mol Biol Cell; 16(2):649-64.

16. Jakowlew SB. 2006.Transforming growth factor-beta in cancer and metastasis. Cancer Metastasis Rev; 25:435-57.

17. Lee SH, Dominguez R. 2010. Regulation of actin cytoskeleton dynamics in cells. Mol. Cells 29, 311-325.

18. McKenzie S, Kyprianou N. 2006. Apoptosis evasion: the role of survival pathways in prostate cancer progression and therapeutic resistance. J Cell Biochem. ; 97(1):18-32.

19. Yilmaz M, Christofori G. 2010. Mechanisms of motility in metastasizing cells. Mol Cancer Res.; 8(5):629-42.

20. DesMarais V, Sidani M, Scemes E, Wang W, Song X, Eddy R, Condeelis J. 2006. Spatial and temporal control of cofilin activity is required for directional sensing during chemotaxis. Curr Biol.; 16(22):2193-205.

21. Micalizzi DS, Wang CA, Farabaugh SM, Schiemann WP, Ford HL. 2010. Homeoprotein Six1 increases TGF-beta type I receptor and converts TGF-beta signaling from suppressive to supportive for tumor growth. Cancer Res. 15; 70(24):10371-80.

22. Noel W. Clarke, Claire A. Hart and Mick D. Brown (2009) Molecular mechanisms of metastasis in prostate cancer. Asian Journal of Andrology 11: 57–67. doi: 10.1038.

23. Oleinik NV, Krupenko NI, Krupenko SA. ALDH1L1 inhibits cell motility via dephosphorylation of cofilin by PP1 and PP2A. 2010. Oncogene. 25; 29(47):6233-44.

24. Ono S. 2007. Mechanism of depolymerization and severing of actin filaments and its significance in cytoskeletal dynamics. Int Rev Cytol; 258.

25. Olson MF. 2008. Applications for ROCK kinase inhibition. Curr Opin Cell Biol.; 20(2):242-8.

26. Sadako Nishimura, Hiroshi Tsuda, Fumio Kataoka ,Tokuzo Arao, Hiroyuki Nomura, Tatsuyuki Chiyoda, Nobuyuki Susumu, Kazuto Nishio, Daisuke Aoki. 2010. Human Pathology; 42:516–521.

27. Steeg PS. 2006. Tumor metastasis: mechanistic insights and clinical challenges". Nature Medicine 12:895-904.

28. Teicher BA. 2007. Transforming growth factor-beta and the immune response to malignant disease. Clin Cancer Res; 13 (21):6247-51.

29. Rainy Umbas, Jack A. Schalken, Tilly W. Aalders, Bob S. Carter,Herbert F. M. Karthaus,Schaafsma, Frans M. J. Debruyne, and William B. Isaacs. 1992. Expression of the Cellular Adhesion Molecule E-Cadherin is reduced or absent in High-Grade Prostate Cancer. Cancer Res; 52; 5104.

30. Van Troys M, Huyck L, Leyman S, Dhaese S, Vandekerkhove J, Ampe C.2008. Ins and outs of ADF/cofilin activity and regulation. Eur J Cell Biol; 87(8-9):649-67.

31. Wang W, Mouneimne G, Sidani M, Wyckoff J, Chen X, Makris A, Goswami S, Bresnick AR, Condeelis JS. 2006. The activity status of cofilin is directly related to invasion, intravasation, and metastasis of mammary tumors; J Cell Biol. 8; 173(3):395-404.

32. Weigang Wang, Robert Eddy, John Condeelis. 2007. The cofilin pathway in breast cancer invasion and metastasis. Nature Reviews Cancer **7**, 429-440.

33. Xu L, Chen YG, Massagué J. 2000. The nuclear import function of Smad2 is masked by SARA and unmasked by TGFbeta-dependent phosphorylation. Nat Cell Biol 2000; (8):559-62.

34. Yilmaz M, Christofori G. 2010. Mechanisms of motility in metastasizing cells. Mol Cancer Res.; 8(5):629-42.

35. Zebda N, Bernard O, Bailly M, Welti S, Lawrence DS, Condeelis. 200. JSPhosphorylation of ADF/cofilin abolishes EGF-induced actin nucleation at the leading edge and subsequent lamellipod extension J Cell Biol. 27; 151 (5):1119-28.